Adsorption (2024) 30:1251–1271
https://doi.org/10.1007/s10450-024-00495-2

Comprehensive Analytical Sorption Thermodynamic (CAST) model for water vapor sorption in cellulosic materials

Mark A. Dietenberger[1] · Samuel V. Glass[1] · Charles R. Boardman[1]

Received: 4 December 2023 / Revised: 9 May 2024 / Accepted: 18 May 2024 / Published online: 9 June 2024

Abstract

Water vapor sorption is a fundamental property of cellulosic materials. Numerous theoretical and empirical models have been developed to describe the relationship between water activity, temperature, and equilibrium moisture content (EMC). However, a meaningful connection between model parameters and thermodynamic properties related to the sorption process is often lacking. In cases where models yield thermodynamic properties, such as through use of the Clausius-Clapeyron equation, these are limited to temperatures where the ideal gas equation is applicable. In this paper we advance a thermodynamic framework and formulate a new semi-empirical sorption model based on the differential Gibbs energy of sorption as a function of EMC and temperature, intended for high temperature applications such as steam drying or fire modeling. We refer to this as the Comprehensive Analytical Sorption Thermodynamic (CAST) model. It has six parameters, includes temperature explicitly, and is invertible. The CAST model includes analytical equations for the differential enthalpy of sorption, the differential entropy of sorption, and the integral heat of wetting. The model is evaluated using sorption data and calorimetric data over a range of temperatures from the wood science literature and compared with several existing models. Overall, the CAST model fits the experimental sorption and calorimetric data with higher accuracy than existing models.

Keywords Wood · Water vapor sorption · Heat of wetting · Differential enthalpy of sorption · Isosteric heat · Equilibrium moisture content

Notation

a_w	Thermodynamic water activity (dimensionless)
a_w^i	Conventional (ideal gas) water activity, i.e., relative humidity (dimensionless)
C	Integration constant
f	Fugacity (Pa or bar)
G	Specific Gibbs energy of the solid (J kg^{-1})
g	Molar Gibbs energy (J mol^{-1})
$\overline{g}_a$	Differential molar Gibbs energy of absorbed water (J mol^{-1})
H	Specific enthalpy of the solid (J kg^{-1})
h	Molar enthalpy (J mol^{-1})
$\overline{h}_a$	Differential molar enthalpy of absorbed water (J mol^{-1})
$K(T)$	Empirical function of temperature for compressibility factor and fugacity coefficient (dimensionless)
$k_1 \ldots k_3$	Constants in equation for compressibility factor and fugacity coefficient
M_w	Molar mass of water (0.018015268 kg mol^{-1})
n	Water content (mol kg^{-1})
P	Total pressure (Pa or bar)
p	Partial vapor pressure or vapor pressure of single component (Pa or bar)
p_c	Critical pressure of water (22.064 MPa)
q_{wet}	Heat of wetting (J kg^{-1})
R	Gas constant (8.314462618 J K^{-1} mol^{-1})
s	Molar entropy (J K^{-1} mol^{-1})
$\overline{s}_a$	Differential molar entropy of absorbed water (J K^{-1} mol^{-1})
T	Temperature (K)
T_c	Critical temperature of water (647.096 K)
u	Moisture content (kg kg^{-1})
V_s	Specific volume of the solid (m^3 kg^{-1})
v	Molar volume (m^3 mol^{-1})
$\overline{v}_a$	Partial molar volume of absorbed water (m^3 mol^{-1})
X	Integration variable for CAST model
Z	Compressibility factor (dimensionless)

✉ Samuel V. Glass
samuel.v.glass@usda.gov

[1] Building and Fire Sciences, US Forest Service Forest Products Laboratory, Madison, WI, USA

Uppercase Greek symbols

Δ	Change in property
${\Delta_\alpha}^\beta y$	Change in property y from phase α to phase β (${\Delta_\alpha}^\beta y = y_\beta - y_\alpha$)

Lowercase Greek symbols

$\alpha_1 \ldots \alpha_6$	Generic fitting parameters
$\beta_1 \ldots \beta_6$	Constants in CAST model
$\gamma_1 \ldots \gamma_3$	Constants in GAB isotherm model
$\delta_1 \ldots \delta_6$	Constants in GAB6 model
$\varepsilon_1, \varepsilon_2$	Constants in ODE4 model
$\zeta_1 \ldots \zeta_4$	Constants in ODP6 model
κ_1, κ_2	Constants in Nelson isotherm model
$\lambda_1 \ldots \lambda_6$	Constants in NA6 model
μ	Chemical potential (J mol^{-1})
ρ	Density (kg m^{-3})
ρ_c	Critical density of water (322 kg m^{-3})
φ	Fugacity coefficient (dimensionless)
$\omega_1 \ldots \omega_3$	Constants in OC3 model

Subscripts

a	Absorbed water
c	Critical value
ds	Dry solid
f	Final value
g	Water vapor (gaseous phase)
gl	Saturated water vapor (gas-liquid equilibrium)
i	Initial value
l	Liquid water
ref	Reference value
s	Solid
w	Water
wet	Wetting

1 Introduction

The properties of cellulosic materials strongly depend on interactions with water. The hygroscopic nature of such materials has important implications for processing and performance across a range of industries, including agricultural products, insulation materials, packaging, pulp and paper, textiles, and wood products. For example, moisture affects the strength and stiffness of wood [1], as well as its physical properties including heat capacity and thermal conductivity [2, 3]. Control of moisture content is necessary to avoid dimensional instability [4, 5], corrosion of embedded metal fasteners [6], surface microbial growth [7–9], and fungal decay [9–11].

Plant–water interactions also strongly influence wildfire behavior [12–14]. Moisture affects the preheating and ignition of forest fuels (live and dead plants) and slows the rates of combustion, fire spread, and heat release. Furthering the fundamental understanding of plant–water relations is necessary to improve the modeling of wildland fire, particularly the influence of moisture on pyrolysis, flame spread, and fire growth [13–17]. Physical models used in these applications need to account for a wide range of conditions that include temperatures above the boiling point and moisture contents from the green condition in live plants to bone dry.

Water can be present in cellulosic materials in the solid, liquid, and vapor phases. In addition, water molecules can be adsorbed on surfaces or taken up within the biopolymer matrix, where they are energetically bound through hydrogen bonds or other intermolecular attractions. We refer to these interactions collectively as absorption. The water vapor sorption isotherm is a fundamental property of hygroscopic materials that relates the equilibrium moisture content (EMC or u, the ratio of the total mass of water in the material to its dry mass) and the relative humidity (RH) or water activity (a_w) at a given temperature (T). Additional factors such as material moisture history and external constraints on moisture-induced swelling may influence the equilibrium state. Equilibrium refers to the condition where the material is neither gaining nor losing moisture. Sorption isotherms are important for understanding plant–water interactions and modeling the material behavior.

An important thermodynamic quantity is the energy involved in absorption of water molecules by a material, or desorption of water molecules from a material. The enthalpy of vaporization of pure water is well known and provides a convenient reference curve as a function of temperature. The enthalpy of water vapor sorption in a material depends not only on temperature but also on the composition of the system, which is usually expressed as material moisture content. Two general approaches exist for quantifying this enthalpy change: calorimetric methods and the analysis of sorption isotherm data across multiple temperatures. The latter is commonly referred to as the isosteric method ("isosteric" meaning constant coverage, originating from the study of adsorption on surfaces, but broadly adapted to mean constant EMC). Because sorption involves equilibrium between two phases, the Clapeyron equation describes the relationship between pressure, temperature, and changes in volume and enthalpy (or entropy) between the phases [18], Ch. 15). The Clapeyron equation, however, is rarely used; typically, the simpler Clausius-Clapeyron equation is used in the literature, which relies on two assumptions. First, the molar volume of absorbed water is assumed to be negligible compared to the molar volume of water vapor. Second, the ideal gas equation is assumed to adequately describe water vapor. Although these assumptions are reasonable at low temperatures and pressures, the Clausius-Clapeyron equation becomes more and more inaccurate as temperature and pressure increase, as demonstrated later in this article.

Numerous equilibrium sorption models have been applied to water vapor sorption in cellulosic materials in the literature [19–27]. These models range from simple empirical equations to theoretical models based on an idealized physical system. Regardless of the type of model, a meaningful connection between model parameters and thermodynamic properties is often lacking. Common theoretical models widely used in the literature, for which the parameters are assumed to represent physical quantities such as changes in enthalpy or Gibbs energy, fail to predict values in agreement with independently measured data for wood [22, 24, 28]. In practice, models often serve merely as EMC/RH fitting equations for the purpose of interpolation prior to applying the Clausius-Clapeyron equation [29–32]. However, use of non-optimal fitting equations for interpolation may bias the subsequent thermodynamic analysis [23, 33–36].

In contrast, a few sorption models have been formulated specifically using empirical relationships between thermodynamic properties and EMC. For example, Anderson and McCarthy [37] developed an isotherm model relating the differential enthalpy of sorption to EMC, and Chung and Pfost [38] and Nelson [39] formulated isotherm models relating the differential Gibbs energy of sorption to EMC. Anderson [12] expanded the model of Nelson [39] with additional parameters such that temperature was included as a variable. This model will be described in detail and evaluated later in this article.

We take a similar approach in this article and develop a sorption model using an empirical relationship between macroscopic thermodynamic properties and EMC. Although our approach does not aim to build a theoretical model from the molecular level or describe all the complex physicochemical phenomena involved in the sorption of water vapor by cellulosic materials [24, 25], this type of model may be useful for accurately simulating heat and moisture transfer in high temperature applications such as steam drying or wildland fire. Prior literature on the thermodynamics of water vapor sorption in cellulosic materials is limited by reliance on the Clausius-Clapeyron equation [23, 33, 35, 39, 40]. Here we advance a thermodynamic framework that overcomes this limitation, adapting the work of Myers and Monson [41] on absolute adsorption of gases in microporous solids. Building on this framework, we develop a semi-empirical sorption model that is valid over a wide range of temperature and pressure conditions. We wanted the model to have the following attributes:

- The model should include temperature explicitly, and the equation giving $u(a_w, T)$ should be readily invertible to give $a_w(u, T)$.
- The model should analytically describe real gas behavior of water vapor in accordance with reference data (i.e., the steam table) between the triple point and the critical point.
- The model should be inherently consistent with the thermodynamics of phase equilibria and specifically include the condition that the chemical potential of water vapor is equal to the chemical potential of absorbed water in the solid material.
- The number of model parameters should be limited, preferably to six or fewer.
- The model should be adaptable to a range of different cellulosic materials.
- The model should fit experimental sorption data accurately over a wide range of temperatures, including the high and low RH regions.
- The model should provide the ability to calculate thermodynamic quantities analytically, including the differential Gibbs energy of sorption, the differential enthalpy of sorption, the differential entropy of sorption, and the integral heat of wetting, with reasonable accuracy in comparison to independent measurements.

Section 2 of this article provides the thermodynamic framework for formulating the model. In Section 3, we describe the Comprehensive Analytical Sorption Thermodynamic (CAST) model, which is based on the differential Gibbs energy of sorption. Section 4 details the methods used for evaluating the model's ability to fit sorption data and calorimetric data from the wood science literature in comparison to several existing models. Section 5 presents results showing the CAST model fits experimental data with higher accuracy than existing models.

2 Thermodynamic framework

Before considering water vapor sorption in hygroscopic materials, we discuss vapor–liquid equilibrium for pure water to provide context on real gas behavior and the effects of temperature.

2.1 Vapor–liquid equilibrium of pure water

The thermodynamics of phase equilibria classically begins with the Clapeyron equation [18, 42, 43], which relates the slope of the saturation pressure vs. temperature curve to differences in entropy and volume between the phases, or alternatively, differences in enthalpy and volume:

$$\frac{\mathrm{d}p_{gl}}{\mathrm{d}T} = \frac{s_{gl} - s_l}{v_{gl} - v_l} = \frac{h_{gl} - h_l}{T\left(v_{gl} - v_l\right)} \tag{1}$$

where p_{gl} is the pressure of the gas phase in equilibrium with the liquid phase, i.e., the saturation vapor pressure (Pa), T is absolute temperature (K), s_{gl} and s_l are the molar entropies of vapor and liquid (J K^{-1} mol^{-1}), v_{gl} and v_l are the molar

volumes of vapor and liquid (m^3 mol^{-1}), and h_{gl} and h_l are the molar enthalpies of vapor and liquid (J mol^{-1}).

The molar enthalpy of vaporization can be expressed as $\Delta_l^g h = h_{gl} - h_l$, where the subscript following the delta symbol indicates the initial phase and the superscript indicates the final phase (this notation is recognized by the International Union of Pure and Applied Chemistry; Cohen et al. [44] p. 60). Standard reference values [45–47], which we subsequently refer to as the steam table, are plotted as the thick light blue curve in Fig. 1 between the triple point (273.16 K) and the critical point (647.096 K). Calculations using Eq. (1) with numerical differentiation of the saturation vapor pressure with respect to temperature based on the empirical equation of Wagner and Pruss [48], and with molar volumes of vapor and liquid calculated using empirical equations for density from Wagner and Pruss [48], give the enthalpy of vaporization to high accuracy (within 0.05% up to 360 °C), yielding the black dotted curve in Fig. 1. These calculations account for real gas behavior that is inherent in the pressure-volume-temperature data of the steam table. Further details are provided in Supplementary Information (SI) Part I.

Real gas behavior can be quantified using the compressibility factor $Z = p_g v_g / RT$, where R is the gas constant (8.31446 J K^{-1} mol^{-1}). The ideal gas equation is equivalent to $Z = 1$. The compressibility factor for saturated water vapor, calculated from the steam table, is plotted in Fig. 2a as a function of temperature. Various functional forms for Z have been proposed based on real gas equations of state [18, 43] or empirical approximations [49]. Here we approximate Z as

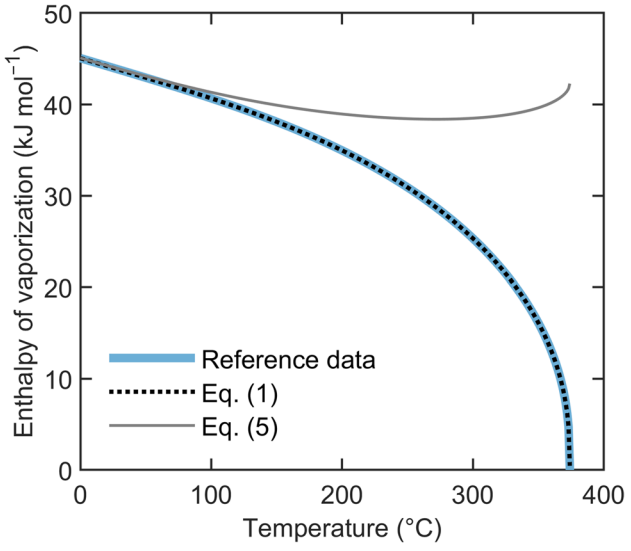

Fig. 1 Enthalpy of vaporization of water as a function of temperature from reference data, Clapeyron equation, and Clausius-Clapeyron equation

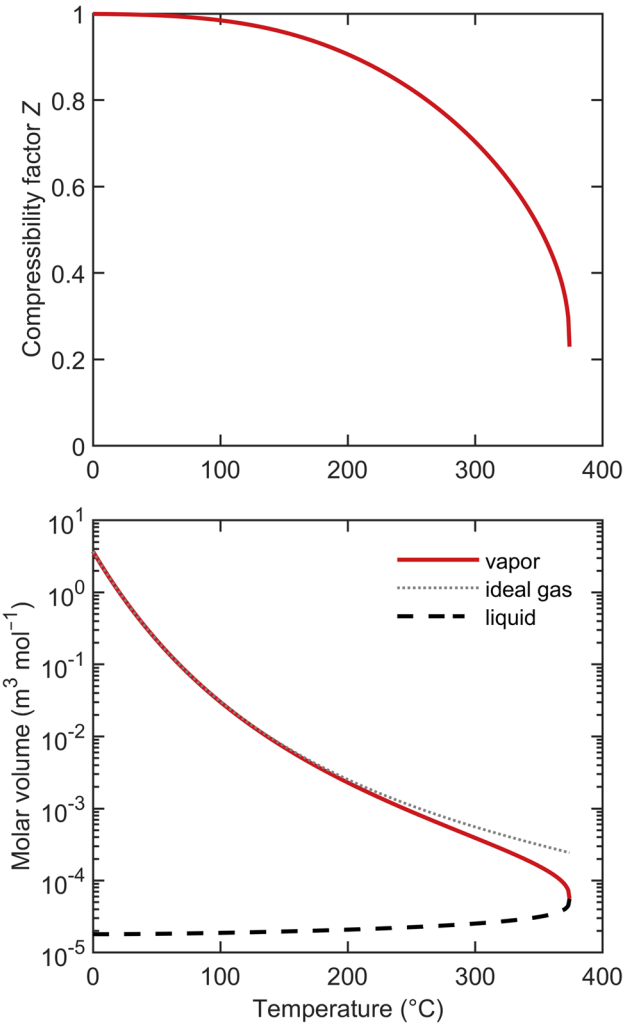

Fig. 2 **a** Compressibility factor of saturated water vapor vs. temperature; **b** molar volume of saturated water vapor and liquid water vs. temperature

$$Z = 1 - \frac{K(T) p_g / p_c}{1 - K(T) p_g / p_c} \tag{2}$$

where $K(T)$ is an empirical function of temperature given below and p_c is the critical pressure of water (22.064 MPa). Equation (2) was proposed previously [50], but we developed a new empirical function for $K(T)$ based on fitting data from the steam table (SI Part I):

$$K(T) = k_1 (T/T_c - k_2)^{-k_3} \tag{3}$$

where T_c is the critical temperature of water (647.096 K) and k_1, k_2, and k_3 are constants (0.186, 0.233, and 2.70, respectively), which were identified by minimizing the sum of squared residuals between the enthalpy of vaporization of water from the steam table and the enthalpy calculated with the Clapeyron equation expressed as

$$\Delta_l^g h = \left(1 - \frac{p_{gl} v_l}{ZRT}\right) \frac{ZRT^2}{p_{gl}} \frac{\mathrm{d}p_{gl}}{\mathrm{d}T} \tag{4}$$

where Z was approximated using Eqs. (2) and (3). The calculated enthalpy of vaporization is accurate to within 0.05% for temperatures up to 318 °C. Across the full range of pressures below saturation, the calculated value of Z is accurate to within 0.2% below 200 °C and to within 1.4% up to 300 °C (SI Part I).

At low temperatures, two simplifications can be made to Eq. (1). First, water vapor can be described using the ideal gas equation ($Z \cong 1$). Second, the molar volume of liquid water can be neglected relative to that of water vapor (Fig. 2b). With these approximations, the Clapeyron equation is reduced to the Clausius-Clapeyron equation:

$$\Delta_l^g h \cong RT^2 \frac{\mathrm{d} \ln p_{gl}}{\mathrm{d}T} \tag{5}$$

This is shown as the gray curve in Fig. 1. At 100 °C, the relative error in the enthalpy of vaporization is only 1.6%, but it increases considerably with temperature.

Another approximation convenient for low temperatures is a linear equation for the enthalpy of vaporization, which gives the saturation vapor pressure through a relatively simple integration of the Clausius-Clapeyron equation [42]. This is described further in SI Part I.

2.2 Water vapor sorption in hygroscopic materials

The literature on thermodynamics of gas sorption in porous solids provides two different approaches, both of which we adapt to describe water vapor sorption in hygroscopic materials. These are based on (i) the Clapeyron equation, which gives the difference in enthalpy between the vapor phase and the absorbed phase, and (ii) the Gibbs energy, which generates a full set of thermodynamic properties. Here we introduce these approaches and show that they are consistent in order to provide the relevant thermodynamic framework for the CAST model in Section 3.

The enthalpy of water vapor varies with pressure and temperature according to the steam table. Figure 3 is a plot of relative enthalpy (h_g/h_{gl}) vs. relative humidity (p_g/p_{gl}) for a series of temperatures. At low temperatures, where water vapor can be described as an ideal gas, $h_g \cong h_{gl}$ across the full range of vapor pressures. Differences between h_g and h_{gl} at low RH become more pronounced with increasing temperature.

The equilibrium between water vapor and absorbed water in a hygroscopic material can be characterized by water vapor pressure, temperature, and composition, which is expressed here either as water content n ($\mathrm{mol_w}$ $\mathrm{kg_{ds}^{-1}}$) or moisture content u ($\mathrm{kg_w}$ $\mathrm{kg_{ds}^{-1}}$, where the subscript "w" refers to water and the subscript "ds" refers to dry solid; $u = n \cdot M_w$, where M_w is the molar mass of water, kg $\mathrm{mol^{-1}}$). The enthalpy of absorbed water varies with n as depicted conceptually in Fig. 4 for constant temperature, in comparison to the states in the pure water system (adapted from Skaar [23] and Nopens et al. [35]). Figure 4 includes the enthalpy of water vapor from Fig. 3 but as a function of n instead of RH. At low temperatures, where water vapor can be described as an ideal gas, h_g would

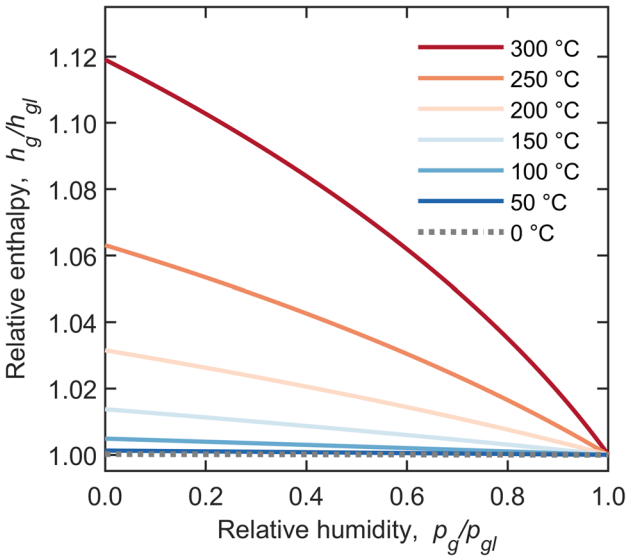

Fig. 3 Enthalpy of water vapor relative to enthalpy at saturation as a function of relative humidity for various temperature series based on the steam table

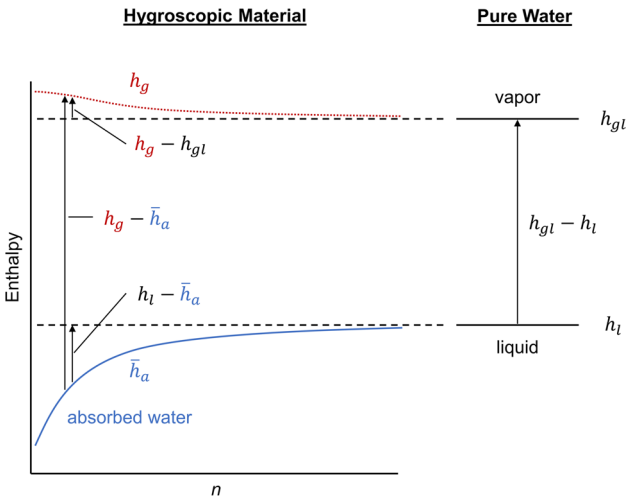

Fig. 4 Conceptual enthalpy diagram showing states of water: (left) water vapor in equilibrium with a hygroscopic material as a function of water content n; (right) pure water system

follow the dashed line rather than the dotted red curve. The enthalpy of absorbed water is properly expressed as a differential quantity [41, 51]: $\overline{h}_a = \left(\frac{\partial H}{\partial n}\right)_T$, where $\overline{h}_a$ is the differential molar enthalpy of absorbed water (J $\mathrm{mol_w^{-1}}$) and H is the total enthalpy of the solid phase (J $\mathrm{kg_{ds}^{-1}}$), which reflects both solid–water interactions and water–water interactions. The bar over the symbol indicates a differential quantity; this distinction is necessary for absorbed water because the differential and integral values are not the same, whereas differential and integral enthalpies are identical for phases with one component (i.e., water vapor and pure liquid water). In general, as the water content approaches the maximum, $h_g \to h_{gl}$ and $\overline{h}_a \to h_l$.

2.2.1 Clapeyron equation

The Clapeyron equation can be applied to multi-component systems such as gas sorption in solids [18, 43, 49]. The change in phase from water vapor to absorbed water is exothermic and therefore has a negative enthalpy change (heat is released from the system). For the sake of continuity with the literature, we use positive quantities (reversing the process and temporarily neglecting sorption hysteresis). Adapting Eq. (1) for absorbed water and introducing Z as was done in Eq. (4), the enthalpy difference can be expressed as

$$\Delta_a{}^g\overline{h} = h_g - \overline{h}_a = (v_g - \overline{v}_a)T\left(\frac{\partial p_g}{\partial T}\right)_n = \left(1 - \frac{\overline{v}_a p_g}{ZRT}\right)\frac{ZRT^2}{p_g}\left(\frac{\partial p_g}{\partial T}\right)_n \tag{6}$$

where v_g is the molar volume of water vapor ($\mathrm{m^3\ mol^{-1}}$), $\overline{v}_a = \left(\frac{\partial \hat{V}_s}{\partial n}\right)_{T,P}$ is the partial molar volume of absorbed water ($\mathrm{m^3\ mol^{-1}}$), V_s is the total specific volume of the solid phase ($\mathrm{m^3\ kg^{-1}}$), and p_g is the water vapor pressure (Pa). This enthalpy difference is also referred to as the *isosteric heat of sorption* in the literature. Equation (6) becomes identical to Eq. (4) in the limiting condition where the water content of the material approaches its maximum, $p_g \to p_{gl}$, and $\overline{v}_a \to v_l$. On the other hand, Eq. (6) reduces to a form of the Clausius-Clapeyron equation when $Z \cong 1$ and $\overline{v}_a \ll v_g$:

$$\Delta_a{}^g\overline{h} \cong RT^2\left(\frac{\partial \ln p_g}{\partial T}\right)_n \tag{7}$$

Note that Eq. (7) becomes identical to Eq. (5) in the limiting condition where the water content of the material approaches its maximum.

2.2.2 Gibbs energy approach

The Gibbs energy can serve as a generating function for other thermodynamic properties. Here we adapt the solution thermodynamics description of gas adsorption in microporous solids [41, 51] for the case of water vapor sorption in hygroscopic materials. We formulate the differential Gibbs energy of sorption based on chemical potential and use it to derive the differential enthalpy of sorption, the differential entropy of sorption, and the integral enthalpy of wetting.

For a constant mass of solid hygroscopic material at constant temperature, the criterion for equilibrium is the equality of the chemical potentials of absorbed water and water vapor: $\mu_a = \mu_g$. We focus first on the gas phase. The equations for thermodynamic properties of a real gas are formulated to resemble those of an ideal gas, but with fugacity instead of pressure. The fugacity f_g (which has units of pressure) is given by $f_g = \varphi p_g$ where φ is the fugacity coefficient, which varies with temperature and pressure. A convenient reference state is pure water at saturation. The chemical potential of water vapor relative to saturation is given by

$$\mu_g - \mu_{gl} = RT\ln\left(\frac{f_g}{f_{gl}}\right) = RT\ln a_\mathrm{w} \tag{8}$$

where $a_\mathrm{w} \equiv f_g/f_{gl}$ is the thermodynamic water activity ([43], p. 279; [44] p. 57). At low temperatures, where $\varphi \to 1$ and $f_g \to p_g$, the thermodynamic water activity is equivalent to the conventional water activity, a_w^i, which is identical to RH expressed as a decimal: $a_\mathrm{w} \cong a_\mathrm{w}^i \equiv p_g/p_{gl}$. The influence of temperature on the ratio $a_\mathrm{w}/a_\mathrm{w}^i = \varphi_g/\varphi_{gl}$ is illustrated in Fig. S6 with calculated values based on the steam table (SI Part I).

Below the critical point, the fugacity coefficient varies approximately linearly with pressure ([18], Fig. 10.2; see SI Part I). We select the following empirical equation for the fugacity coefficient:

$$\varphi = 1 - K(T)\frac{p_g}{p_c} \tag{9}$$

where $K(T)$ is given by Eq. (3). Equation (9) for φ is consistent with Eq. (2) for Z, as shown in SI Part I.

An independent method of obtaining the chemical potential of water vapor μ_g, for the purpose of evaluating the adequacy of Eq. (9), is by way of the steam table, noting its equivalence to the molar Gibbs energy of water vapor g_g (J $\mathrm{mol^{-1}}$):

$$\mu_g = g_g = h_g - Ts_g \tag{10}$$

where h_g is the molar enthalpy (J $\mathrm{mol^{-1}}$) and s_g is the molar entropy of water vapor (J $\mathrm{K^{-1}\ mol^{-1}}$). Calculated values of $\mu_g - \mu_{gl}$ from Eq. (8), with φ from Eq. (9) and $K(T)$ from Eq. (3), agree with $g_g - g_{gl}$ from the steam table to within

0.18% at 200 °C, 0.44% at 250 °C, and 1.2% at 300 °C (SI Part I). This demonstrates the validity of the approximation for the fugacity coefficient up to 300 °C and confirms the equivalence of the chemical potential (calculated using fugacity) and the molar Gibbs energy of water vapor (calculated from molar enthalpy and entropy from the steam table) for the subcritical region.

For a constant mass of solid hygroscopic material, the chemical potential (J mol^{-1}) of absorbed water is

$$\mu_a = \left(\frac{\partial G}{\partial n}\right)_{T,P} \tag{11}$$

where G is the total Gibbs energy of the solid phase (J kg_{ds}^{-1}) and the partial derivative is at constant temperature and total pressure. The differential Gibbs energy of sorption is expressed as a positive quantity (with a sign change) as $\Delta_a{}^l\overline{g} = \mu_l - \mu_a$ where μ_l is the chemical potential of pure liquid water. Recalling that $\mu_a = \mu_g$ for equilibrium between water vapor and absorbed water in the hygroscopic material, and $\mu_l = \mu_{gl}$ for vapor–liquid equilibrium of pure water, the differential Gibbs energy of sorption can be related to thermodynamic water activity from Eq. (8):

$$\Delta_a{}^l\overline{g} = -RT \ln a_w \tag{12}$$

The differential enthalpy of sorption, $\Delta_a{}^l\overline{h}$, can be generated from $\Delta_a{}^l\overline{g}$ as follows. For a process at constant total pressure, the Gibbs-Helmholtz relation links the change in enthalpy to the change in Gibbs energy [18, 43]:

$$\Delta h = -T^2\left[\frac{\partial(\Delta g/T)}{\partial T}\right]_P \tag{13}$$

Because $\Delta_a{}^l\overline{g}$ is a function of n, the partial derivative is taken at constant P and n:

$$\Delta_a{}^l\overline{h} = h_l - \overline{h}_a = -T^2\left[\frac{\partial\left(\Delta_a{}^l\overline{g}/T\right)}{\partial T}\right]_{P,n} = -T^2\left(\frac{\partial\left[\left(-RT\ln a_w\right)/T\right]}{\partial T}\right)_{P,n} = RT^2\left(\frac{\partial \ln a_w}{\partial T}\right)_{P,n} \tag{14}$$

A full derivation of this equation is given in SI Part II. At low temperatures, a_w in Eq. (14) can be considered equivalent to a_w^i (RH expressed as a decimal). This enthalpy difference is also referred to as the *net isosteric heat of sorption* or the *differential heat of wetting* in the literature.

Given the equations for $\Delta_a{}^l\overline{g}$ and $\Delta_a{}^l\overline{h}$ above, the differential entropy of sorption, $\Delta_a{}^l\overline{s}$, can be calculated using $\Delta_a{}^l\overline{g} = \Delta_a{}^l\overline{h} - T\Delta_a{}^l\overline{s}$.

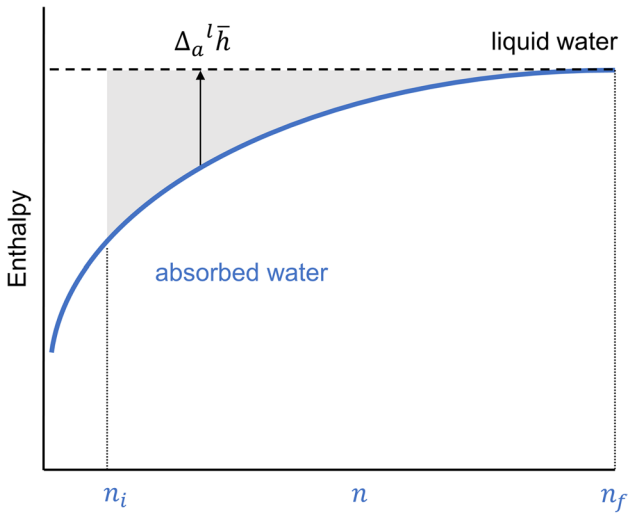

Fig. 5 Conceptual enthalpy diagram showing absorbed water in a hygroscopic material as a function of water content n; the shaded area corresponds to the heat of wetting

In addition to these differential quantities, the integral enthalpy of wetting can be generated as follows. Consider the process of water absorption in a hygroscopic material from an initial equilibrium state with water content n_i (mol_w kg_{ds}^{-1}). Liquid water is added such that the material becomes fully water-saturated, with final water content n_f. The heat released by the (exothermic) absorption process can be measured with a calorimeter [23, 35]. For convenience, we express this heat of wetting (and the corresponding integral enthalpy) as a positive quantity with the symbol q_{wet} (J kg_{ds}^{-1}), which is related to the differential enthalpy of sorption by

$$q_{wet} = \int_{n_i}^{n_f} \Delta_a{}^l\overline{h}\, dn \ \ (\text{constant } T) \tag{15}$$

The magnitude of the heat of wetting depends on the initial water content. This relationship is depicted graphically in Fig. 5, where the heat of wetting corresponds to the area of the shaded region. For the case where the material is initially completely dry, the total heat of wetting (J kg_{ds}^{-1}) is found by integrating Eq. (15) from $n_i = 0$. The rigorous definitions of differential and integral thermodynamic quantities from this framework are used in the development of the CAST model in Section 3.

2.2.3 Equivalence of the Clapeyron equation and the Gibbs energy approach

Two different thermodynamic approaches for water vapor sorption in hygroscopic materials were described above:

(i) the Clapeyron equation (Section 2.2.1), which gives the difference in enthalpy between the vapor phase and the absorbed phase, and (ii) the Gibbs energy approach (Section 2.2.2). The equivalence of these approaches was explored for two cases. First, for the limiting condition of absorbed water in a hygroscopic material approaching its maximum water content, the isosteric heat of sorption approaches the enthalpy of vaporization of water. In SI Part III the calculated enthalpy using the Clapeyron equation is shown to be equivalent to that based on the Gibbs energy, or solution thermodynamics approach, both accurate to within 0.05% of the steam table up to 318 °C.

Second, in SI Part IV the sorption data of Engelhardt [52] for beech between 110 °C and 170 °C, over a wide range of RH values, is analyzed using both approaches. The results confirm that the enthalpy values calculated with the two approaches agree to within 0.2%.

3 CAST model formulation

In this section we introduce a new equilibrium sorption model formulated with the differential Gibbs energy of sorption ($\Delta_a{}^l\overline{g}$) as a function of moisture content and temperature. Additional thermodynamic quantities are generated from $\Delta_a{}^l\,\overline{g}$, including $\Delta_a{}^l\overline{h}$, $\Delta_a{}^l\overline{s}$, and q_{wet}. Subsequently we simplify the notation by dropping the "*a*" and "*l*."

An approximately linear relationship between the logarithm of $\Delta\overline{g}$ and EMC at constant temperature was reported in previous work for wood, cellulose, and agricultural products [38, 39]. EMC is given the symbol u ($\text{kg}_\text{w}\ \text{kg}_\text{ds}^{-1}$). This can be expressed as

$$\Delta\overline{g}(u) = \alpha_1 \exp\left(-\alpha_2 u\right) \tag{16}$$

where α_1 and α_2 are positive fitting parameters.

The CAST model builds on this concept of $\Delta\overline{g}(u,T)$ but differs from earlier models in two key aspects. First, it accounts for real gas behavior using the thermodynamic framework of Section 2. Second, it uses a different functional form for $\Delta\overline{g}(u,T)$. Figure 6 is a semi-log plot of $\Delta\overline{g}$ vs. u based on sorption isotherm data for different cellulosic materials; the points were calculated with Eq. (12) using measured vapor pressures and temperatures. The gray dashed line, which represents earlier models [38, 39], clearly does not fit the data adequately across the full range of EMC values. At a given temperature, the following equation provides an improved fit, plotted as the blue curve in Fig. 6:

$$\Delta\overline{g}(u) = \left(\alpha_3 u + \alpha_4\right)^{-\alpha_5} - \alpha_6 \tag{17}$$

where $\alpha_3 \ldots \alpha_6$ are positive fitting parameters (Table 1). The form of this equation is an empirical modification of the isotherm model of Halsey [53] with two additional parameters that allow the curve to fit the data more closely. By fitting data at multiple temperatures, we find that α_3 varies with temperature, but α_4, α_5, and α_6 can be considered constants. The temperature dependence of α_3 can be described by $\alpha_3(T) = \beta_1 e^{-\beta_2/T} + \beta_3$, where β_1, β_2, and β_3 are positive constants. The term $\beta_1 e^{-\beta_2/T}$ resembles the Arrhenius equation used for describing rates of chemical reactions; this form has been used previously in a modification of the Guggenheim-Anderson-de Boer isotherm model [54].

Combining these equations, the CAST model is formulated as

$$\Delta\overline{g}(u,T) = \left[u\left(\beta_1 e^{-\beta_2/T} + \beta_3\right) + \beta_4\right]^{-\beta_5} - \beta_6 \tag{18}$$

where $\beta_1 \ldots \beta_6$ are positive constants. This formulation focuses on the properties of absorbed water in the hygroscopic material. Following the pattern of Section 2.2.2, we use $\Delta\overline{g}(u,T)$ as a generating function for additional thermodynamic properties below.

The differential enthalpy of sorption is derived by applying the Gibbs-Helmholtz relation (Eq. 13) to (18):

$$\Delta\overline{h}(u,T) = \Delta\overline{g} + \left(\frac{\Delta\overline{g} + \beta_6}{T}\right)\left[\frac{u\beta_1\beta_2\beta_5 e^{-\beta_2/T}}{u\left(\beta_1 e^{-\beta_2/T} + \beta_3\right) + \beta_4}\right] \tag{19}$$

We note the relative simplicity of this equation, which comes from using only two empirical constants (β_1 and β_2) for the temperature dependence of the differential Gibbs energy.

The differential entropy of sorption is given by

$$\Delta\overline{s}(u,T) = \frac{\Delta\overline{h} - \Delta\overline{g}}{T} = \left(\frac{\Delta\overline{g} + \beta_6}{T^2}\right)\left[\frac{u\beta_1\beta_2\beta_5 e^{-\beta_2/T}}{u\left(\beta_1 e^{-\beta_2/T} + \beta_3\right) + \beta_4}\right] \tag{20}$$

The heat of wetting is related to the differential enthalpy of sorption through Eq. (15). Adapting this for u in place of n ($u = n \cdot M_\text{w}$, where M_w is the molar mass of water), we have.

$$q_{\text{wet}} = \frac{1}{M_\text{w}} \int_{u_i}^{u_f} \Delta\overline{h}\, \text{d}u \quad (\text{constant}\, T) \tag{21}$$

This quantity can be calculated by analytically integrating Eq. (19), which is more convenient by defining a new variable X as

$$X = u\left(\beta_1 e^{-\beta_2/T} + \beta_3\right) + \beta_4 \tag{22}$$

Substitution of Eq. (22) into Eq. (18) gives the differential Gibbs energy of sorption as

$$\Delta\overline{g} = X^{-\beta_5} - \beta_6 \tag{23}$$

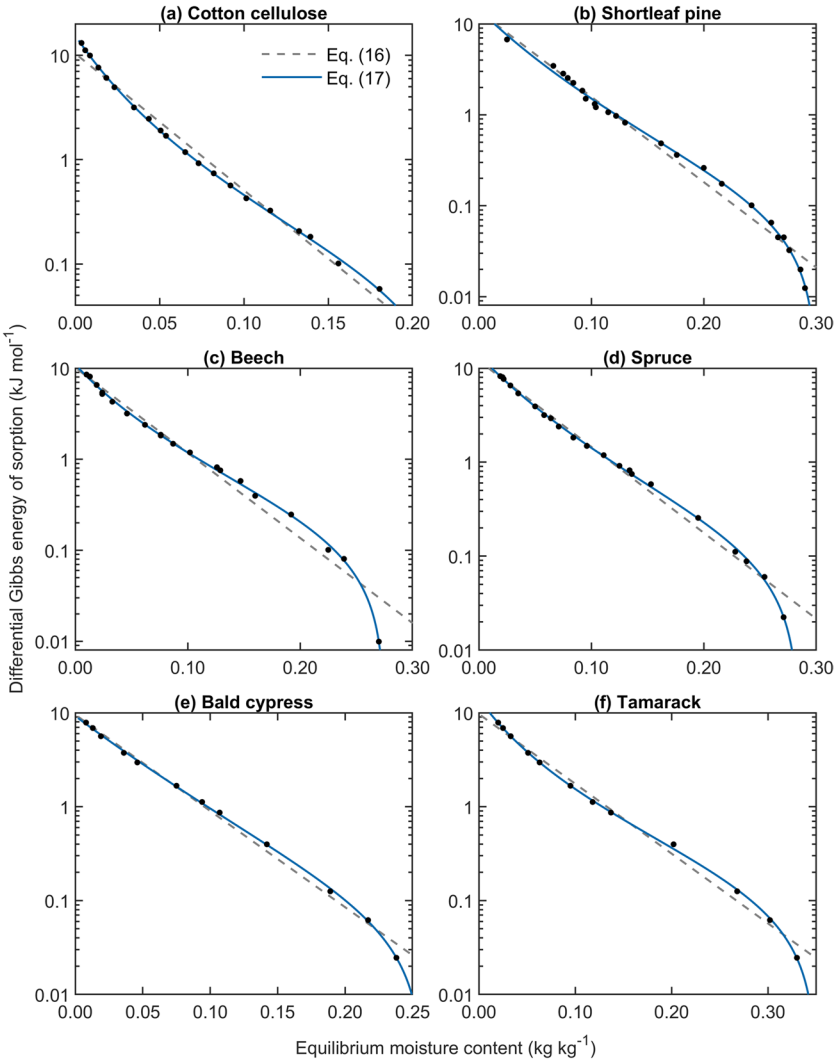

Fig. 6 Differential Gibbs energy of sorption vs. equilibrium moisture content of **a** cotton cellulose at 25 °C [55]; **b** shortleaf pine sapwood at 25 °C [56]; **c** beech and **d** spruce at 25 °C [57]; **e** bald cypress and **f** tamarack at 21 °C [58]

Combining these equations, the heat of wetting is given by the following formula:

$$q_{\text{wet}} = \frac{1}{M_{\text{w}}\left(\beta_1 e^{-\beta_2/T} + \beta_3\right)} \left[\frac{X^{1-\beta_5}}{1-\beta_5} - \beta_6 X + \left(\frac{\beta_1\beta_2\beta_5 e^{-\beta_2/T}}{T\left(\beta_1 e^{-\beta_2/T} + \beta_3\right)} \right) \left(\frac{X^{1-\beta_5}}{1-\beta_5} - \frac{\beta_4 X^{-\beta_5}}{\beta_5} \right) \right]_{X_i}^{X_f} \tag{24}$$

Table 1 Parameter values for Eq. (17) fitted to experimental data in Fig. 6 (with u in kg kg^{-1} and $\Delta\, g$ in kJ mol^{-1})

Material	α_3	α_4	α_5	α_6
Cotton cellulose	7.112	0.478	3.721	0.066
Shortleaf pine	3.230	0.585	4.995	0.110
Beech	4.565	0.432	2.879	0.221
Spruce	3.708	0.524	4.083	0.154
Bald cypress	1.904	0.808	10.429	0.065
Tamarack	4.510	0.364	2.631	0.173

Here X_i is calculated from u_i with Eq. (22). As EMC approaches its maximum, $a_w \to 1$ and $\Delta\overline{g} \to 0$. For calculating the heat of wetting by integration, it is necessary to extrapolate the model to a final value u_f and corresponding value X_f where $\Delta\overline{g} = 0$. From Eq. (23) this value is $X_f = \beta_6{}^{-1/\beta_5}$, which combined with Eq. (22) gives the extrapolated EMC:

$$u_f(T) = \frac{{\beta_6}^{-1/\beta_5} - \beta_4}{\beta_1 e^{-\beta_2/T} + \beta_3} \tag{25}$$

This extrapolated value corresponds to the point where $\Delta\overline{g} = 0$, $a_w = 1$, and $q_{wet} = 0$.

In addition to the thermodynamic properties of absorbed water in a hygroscopic material given above, the CAST model describes water vapor by connecting $\Delta\overline{g}(u,T)$ in Eq. (18) with $\Delta\overline{g} = -RT \ln a_w$ (see Eq. 12). Solving for u leads to an equilibrium sorption model:

$$u = \frac{\left(-RT \ln a_w + \beta_6\right)^{-1/\beta_5} - \beta_4}{\beta_1 e^{-\beta_2/T} + \beta_3} \tag{26}$$

This equation can be inverted to give the thermodynamic water activity:

$$a_w = \frac{\varphi_g p_g}{\varphi_{gl} p_{gl}} = \exp\left[\frac{-\Delta\overline{g}(u,T)}{RT}\right] = \exp\left\{\frac{-\left[u\left(\beta_1 e^{-\beta_2/T} + \beta_3\right) + \beta_4\right]^{-\beta_5} + \beta_6}{RT}\right\} \tag{27}$$

This results in a parabolic equation for the water vapor pressure p_g after substitution of the empirical expression for the fugacity coefficient from Eq. (9). Solving the parabolic equation completes the analytical inversion process.

Equations (18), (19), (24), (26), and (27) thus allow calculation of quantities that can be compared with experimentally determined values. The model is intended for general application to cellulosic materials for RH levels of 0.995 and below. It is not intended for modeling EMC in the over-hygroscopic region because materials differ considerably in pore volume distribution. In materials such as wood the EMC increases dramatically at higher RH levels with capillary water [25, 59]. The extrapolated values u_f and X_f given above should not be interpreted as being physically significant; they are not intended for comparison with any experimentally determined values. Nevertheless, the form of the equation for u_f provides a convenient way of normalizing the EMC. Combining Eqs. (25) and (26) yields

$$\frac{u}{u_f} = \frac{\left(-RT \ln a_w + \beta_6\right)^{-1/\beta_5} - \beta_4}{{\beta_6}^{-1/\beta_5} - \beta_4} \tag{28}$$

This normalized EMC from the CAST model is a function of $-RT \ln a_w$ alone; this dependence was shown previously by Willems [60] across several datasets for water vapor sorption in wood.

4 Model evaluation methods

This section documents the selection of experimental data from the literature, the additional sorption models used for comparison, and the optimization methods used for fitting the data.

4.1 Literature data selection

Zelinka et al. [61] evaluated literature on water vapor sorption measurements in wood at multiple temperatures up to 100 °C to identify datasets that could be used for thermodynamic analysis and testing equilibrium sorption models. They evaluated data quality based on several criteria: the stringency involved in determining when specimens reached equilibrium, often stated as a threshold for change in mass with time; measurement uncertainty for moisture content, temperature, and relative humidity; and stability of temperature and relative humidity conditions. From the datasets considered most reliable by Zelinka et al. [61], the data of Weichert [57] for spruce and beech covered the widest range of temperatures. This dataset was used as digitized by Zelinka et al. [61]. The literature on sorption data at temperatures above 100 °C has not been evaluated with the same level of detail, though Pearson et al. [62] highlighted the experimental challenges involved and the discrepancies between different publications with increasing temperature. To supplement the data of Weichert at temperatures above 100 °C, we included data for beech from Engelhardt [52], which we digitized from the published plot of EMC vs. RH data points at 110–170 °C. In addition, Engelhardt [52] provided a measured sorption curve for beech at 20 °C (though discrete points were not provided); this curve closely matches the beech data of Weichert [57] at 25 °C (SI Part IV).

Calorimetric data for the same wood species is sparse and limited to the low temperature range. We selected the heat of wetting data of Volbehr [63] for spruce and Hearmon and Burcham [64] for beech. The former was taken from tabulated values of q_{wet} and initial moisture content, u_i. For the latter, the measured data points were not reported; instead, the published plot of q_{wet} vs. u_i had curves drawn by hand to best represent the data. We thus estimated discrete values from the original curves at u_i intervals of 0.01 kg kg^{-1}. In addition, we selected calorimetric data for beech

Table 2 Synopsis of experimental data from the literature used in model evaluation

Type of measurement	Reference	Wood	Temperature (°C)	RH range or initial EMC (u_i) range
Sorption isotherm	Weichert [57]	Unspecified spruce, unspecified beech	25, 50, 75, 100	RH: 0.02–0.99 (absorption)
	Engelhardt [52]	Beech (*Fagus sylvatica* L.)	110, 130, 150, 170	RH: 0.10–0.96 (absorption)
Heat of wetting	Volbehr [63]	Unspecified spruce	0	u_i: 0.003–0.277 kg kg^{-1}
Heat of wetting	Hearmon and Burcham [64]	Unspecified beech	17, 28, 39, 47, 61, 71	u_i: 0–0.25 kg kg^{-1}
Heat of wetting	Nopens et al. [35]	Beech (*Fagus sylvatica* L.)	25[a]	u_i: 0–0.20 kg kg^{-1}
Sorption calorimetry (differential enthalpy)	Nopens et al. [35]	Beech (*Fagus sylvatica* L.)	25	RH: 0–0.80 (absorption)

[a]Temperature not specified; 25 °C assumed based on related measurements

from Nopens et al. [35] for both heat of wetting measured by solution calorimetry and differential enthalpy measured by sorption calorimetry. Heat of wetting was digitized from the published plot of q_{wet} vs. u_i. Differential enthalpy of sorption (referred to in the original as "mixing enthalpy") was obtained from the authors, and mean values of three replicates at intervals of 0.01 kg kg^{-1} were calculated. Relevant details of the various datasets are summarized in Table 2.

For consistency, all sorption data included here were measured in absorption (starting from a dry initial condition), and heat of wetting data were either initially dry or conditioned to an initial EMC by absorption. Desorption is not considered in this evaluation, but the model is expected to have the versatility to fit both absorption and desorption data, which will be examined in future work.

In addition to these primary datasets, we consider the calculated differential enthalpy of sorption from Weichert [65], who applied the Clausius-Clapeyron equation to his sorption data for spruce and beech (25–100 °C). We also draw comparisons with the influence of temperature on the total heat of wetting measured by Kelsey and Clarke [66] for Klinki pine and by Kajita [67] for Hinoki.

The effects of swelling pressures within the wood cell wall on the thermodynamics of sorption are implicitly included in the experimental data summarized above. It is important to note that the thermodynamic framework underlying the CAST model assumes a system at constant total pressure. Measurements of the heat of wetting described above were conducted at atmospheric pressure, so this condition is met. However, water vapor sorption measurements were not strictly at constant total pressure but included a range of pressures from partial vacuum at 25–100 °C [57] to well above atmospheric pressure at higher temperatures [52]. The influence of external pressure is further discussed in SI Part V, which shows that the effect of this range of pressures on the sorption data and differential enthalpy of sorption is negligible.

4.2 Other sorption models

Several additional equilibrium sorption models were fitted to the same datasets described above. The models are described briefly below with full details in SI Part VI.

4.2.1 Modified Guggenheim-Anderson-de Boer model (GAB6)

The original GAB model, named after Guggenheim [68], Anderson [69], and de Boer [70] is a three-parameter isotherm equation. This model has been widely used for cellulosic materials including agricultural products, paper, textiles, and wood [19, 20, 24, 54, 71, 72]. The GAB model was derived from an idealized view of multilayer adsorption of molecules on the surface of an adsorbent. It was modified to include temperature explicitly, for example, by Weisser [54], where each model parameter was expanded with a form resembling Arrhenius reaction kinetics. The parameters of the original model have been identified with physical quantities in previous literature (e.g., number of sorption sites and enthalpy values). However, Thybring et al. [24] demonstrated that the model-predicted values are not valid for water vapor sorption in wood. We therefore treat the parameters as empirical coefficients and express the model as follows:

$$u = \frac{\gamma_1\gamma_2\gamma_3 a_w}{\left(1-\gamma_3 a_w\right)\left[1+\left(\gamma_2-1\right)\gamma_3 a_w\right]}, \text{with } \gamma_1 = \delta_1 e^{\delta_2/T}; \gamma_2 = \delta_3 e^{\delta_4/T}; \gamma_3 = \delta_5 e^{\delta_6/T} \quad (29)$$

where $\delta_1 \ldots \delta_6$ are fitting parameters. We refer this as the GAB6 model.

4.2.2 Modified Nelson model (NA6)

The original model of Nelson [39] is a two-parameter isotherm equation formulated with the natural logarithm of $\Delta\bar{g}$ as a linear function of EMC, with $\Delta\bar{g}$ related to RH using the ideal gas equivalent of Eq. (12). Anderson [12] modified this model to include temperature explicitly, expanding each parameter as a second order polynomial function of temperature:

$$\ln \Delta\bar{g} = \kappa_1 + \kappa_2 u, \text{with } \kappa_1 = \lambda_1 + \lambda_2 T + \lambda_3 T^2; \kappa_2 = \lambda_4 + \lambda_5 T + \lambda_6 T^2 \tag{30}$$

where $\lambda_1 \ldots \lambda_6$ are fitting parameters. The abbreviation "NA6" is used for this model based on the names Nelson & Anderson and the number of parameters. The original and modified forms have been applied to wood, cellulose, and foliar materials in fire modeling [12–14, 23, 39]. Although the original models assumed ideal gas behavior, which was suitable for the temperature ranges considered, here we use thermodynamic water activity and express the model as

$$\begin{aligned} a_w &= \exp\left(\frac{-\Delta\bar{g}}{RT}\right) = \exp\left\{\frac{-\exp[\kappa_1 + \kappa_2 u]}{RT}\right\} \\ &= \exp\left\{\frac{-\exp\left[\lambda_1 + \lambda_2 T + \lambda_3 T^2 + (\lambda_4 + \lambda_5 T + \lambda_6 T^2)u\right]}{RT}\right\} \end{aligned} \tag{31}$$

4.2.3 Modified Oswin model (OC3)

The original model of Oswin [73] is a two-parameter isotherm equation. It was modified to include temperature explicitly [74] and has been applied to a variety of materials including foods [20, 33, 75, 76], wood [77], and a cellulosic membrane [78]. The abbreviation "OC3" is used for this model based on the names Oswin & Chen and the number of fitting parameters. Water activity is given by

$$a_w = \frac{1}{1 + \left(\frac{\omega_1 - \omega_2 T}{u}\right)^{\omega_3}} \tag{32}$$

where ω_1, ω_2, and ω_3 are positive fitting parameters.

4.2.4 Models derived from Othmer's postulate (ODE4 and ODP6)

The differential enthalpy of sorption (relative to liquid water) at low temperatures can be obtained from the slope of a log-log plot of RH for constant EMC at different temperatures vs. saturation vapor pressure of pure water. This method, based on the work of Othmer [79, 80], has been widely used to determine the differential enthalpy of sorption of water vapor in cellulosic materials [40, 81–84]. Othmer postulated that the ratio $\Delta\bar{h}/\Delta_l^g h$ is dependent only on EMC (that is, invariant with temperature). However, Othmer's method gives appreciable errors compared to the Clapeyron equation for analysis of high-temperature sorption data because it assumes ideal gas behavior (SI Part IV).

We derive two sorption models based on this postulate (SI Part VI), using a linear equation for $\Delta_l^g h$ and two different functional forms for the EMC dependence of $\Delta\bar{h}$. The first form is an exponential decay function, which gives the following model:

$$a_w = \exp\left\{-\frac{C}{RT_{ref}} - \varepsilon_1 \exp(-\varepsilon_2 u)\left[\frac{L_0}{RT} - \frac{L_0}{RT_{ref}} + \frac{L_1}{R}\ln\left(\frac{T}{T_{ref}}\right)\right]\right\} \tag{33}$$

where ε_1, ε_2, C, and T_{ref} are fitting parameters and L_0 and L_1 are constants related to $\Delta_l^g h$. The abbreviation "ODE4" is used for this model based on the names Othmer & Dietenberger, the exponential form, and the number of fitting parameters.

The second form is a power-law function, which gives the following model:

$$a_w = \exp\left\{-\frac{C}{RT_{ref}} - \left[\zeta_1 (u + \zeta_2)^{-\zeta_3} + \zeta_4\right]\left[\frac{L_0}{RT} - \frac{L_0}{RT_{ref}} + \frac{L_1}{R}\ln\left(\frac{T}{T_{ref}}\right)\right]\right\} \tag{34}$$

where $\zeta_1 \ldots \zeta_4$, C, and T_{ref} are fitting parameters and L_0 and L_1 are constants related to $\Delta_l^g h$. The abbreviation "ODP6" is used for this model based on the names Othmer & Dietenberger, the power-law form, and the number of fitting parameters.

The inverted forms of these models, equations for differential enthalpy of sorption and heat of wetting, and further details are given in SI Part VI.

4.3 Model optimization

Two different approaches were used for fitting experimental data and identifying model parameters. Goodness of fit was quantified using the coefficient of determination (R^2). The first approach maximized only $R^2(u)$ to test whether fitting EMC alone gives accurate predictions of other quantities, such as heat of wetting and differential enthalpy of sorption. The second approach maximized the weighted average R^2 across multiple quantities, to assess the ability of the models to simultaneously fit all the data. Weighting factors were selected to maintain good fitting of EMC values while improving the fitting of the other quantities. Weighting factors were set to 1 for sources with data at multiple temperatures, i.e., sorption data [52, 57] and heat of wetting data of Hearmon and Burcham [64]. Weighting factors were set

to 0.1 for sources with data at a single temperature, i.e., $\Delta\overline{h}$ values of Weichert [65] and calorimetry data of Volbehr [63] and Nopens et al. [35].

For both approaches, the generalized reduced gradient method was used in the Excel Solver (Microsoft Corp., Redmond, WA, USA). Different sets of initial parameter values were explored to avoid possible local minima.

5 Model evaluation results and discussion

The first approach (optimizing only EMC) yielded higher values of R^2 for the six-parameter models (CAST, GAB6, NA6, and ODP6) than the three- and four-parameter models (OC3 and ODE4). Details are provided in SI Part VII (Tables S6 and S7). Values of $R^2(u)$ and $R^2(a_w)$ for the CAST, GAB6, and ODP6 models were in the range 0.995–0.999, with the NA6 model having slightly lower values. In general, the fitting of the heat of wetting and differential enthalpy of sorption were inadequate when the models were optimized only to EMC data. Nonetheless, the CAST model gave the best results for q_{wet} and Δh for this approach, although q_{wet} was systematically underpredicted and mean relative errors for both quantities were in the range 7–27% across the different wood species and data sources. Given this finding, we focus on the second optimization approach below (simultaneously fitting u, a_w, q_{wet}, and $\Delta\overline{h}$).

Table 3 Parameter values of the CAST model fitted to sorption and calorimetric data (with u in kg kg^{-1}, T in K, and $\Delta\overline{g}$ in kJ mol^{-1})

Parameter	Beech	Spruce
β_1	46.33	304.2
β_2	777.6	1661
β_3	2.028	3.520
β_4	0.2210	0.3895
β_5	1.725	2.886
β_6	0.3664	0.2006

5.1 Overview

The optimized CAST model parameters are listed in Table 3. Values of R^2 for the various models are reported in Tables 4 and 5 based on each set of experimental data. Overall, these fitting statistics indicate that the CAST model represents the sorption data and related thermodynamic quantities exceptionally well. Although the experimental datasets for beech and spruce are taken from disparate publications spanning from 1896 to 2019, they are unified effectively by the CAST model coupled with the improved thermodynamic framework. For example, the beech data include sorption isotherm measurements from two publications covering the range 25–170 °C [52, 57], heat of wetting data from two publications [35, 64], and sorption calorimetry data directly giving the differential enthalpy [35]. It is interesting to note that the CAST model provides a close link between the spruce dataset of Volbehr [63], which is considered the first publication

Table 4 Coefficient of determination (R^2) for various models fitted to beech data

Quantity	Data source	CAST	GAB6	NA6	OC3	ODE4	ODP6
u	Weichert [57]	0.995	0.995	0.974	0.792	0.941	0.986
	Engelhardt [52]	0.997	0.996	0.983	0.844	0.863	0.968
a_w	Weichert [57]	0.998	0.994	0.995	0.955	0.963	0.994
	Engelhardt [52]	0.994	0.988	0.977	0.891	0.880	0.970
$\Delta\overline{g}$	Weichert [57]	0.988	-	0.962	-	0.923	0.969
	Engelhardt [52]	0.975	-	0.908	-	0.715	0.903
q_{wet}	Hearmon and Burcham [64]	0.996	0.990	0.986	0.825	0.853	0.975
	Nopens et al. [35]	0.934	0.903	0.938	0.822	0.869	0.960
$\Delta\overline{h}$	Weichert [65]	0.990	0.956	0.946	0.716	0.903	0.982
	Nopens et al. [35]	0.962	0.923	0.934	0.875	0.800	0.745

Table 5 Coefficient of determination (R^2) for various models fitted to spruce data

Quantity	Data source	CAST	GAB6	NA6	OC3	ODE4	ODP6
u	Weichert [57]	0.998	0.992	0.993	0.947	0.978	0.994
a_w	Weichert [57]	0.999	0.993	0.996	0.971	0.985	0.994
$\Delta\overline{g}$	Weichert [57]	0.992	-	0.979	-	0.919	0.967
q_{wet}	Volbehr [63]	0.999	0.957	0.994	0.855	0.887	0.987
$\Delta\overline{h}$	Weichert [65]	0.998	0.959	0.995	0.929	0.925	0.914

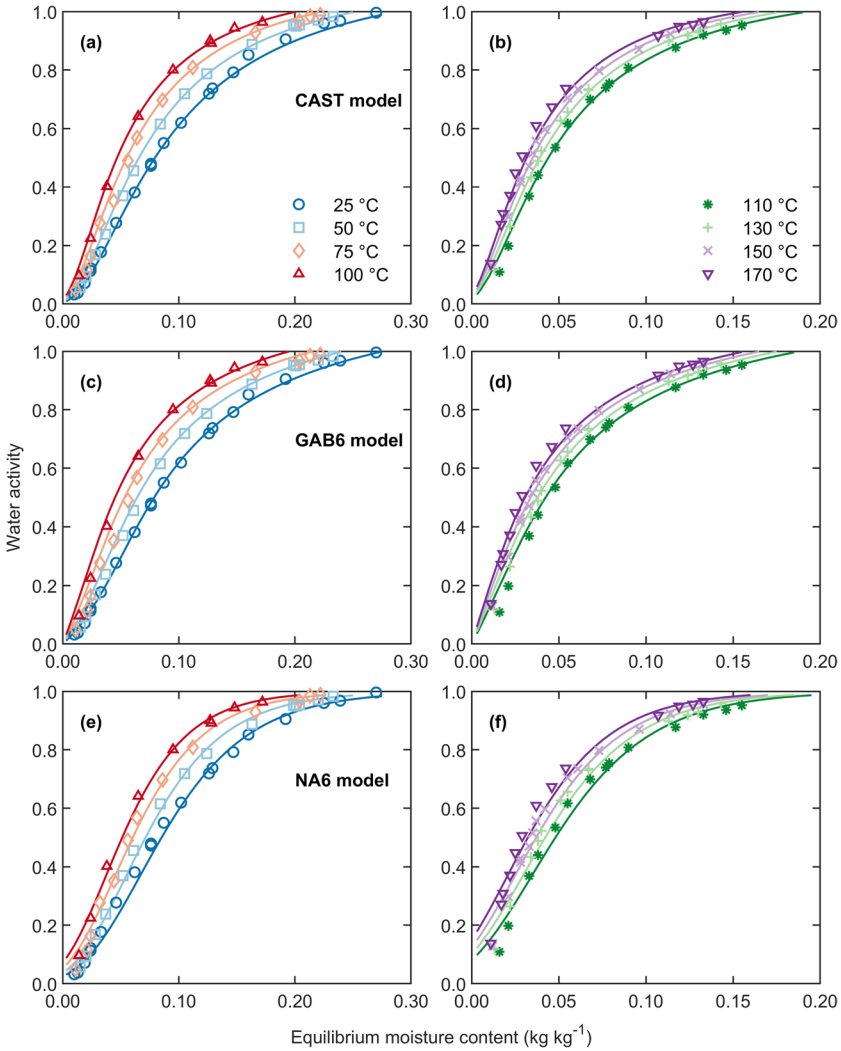

Fig. 7 Fits of select models (solid curves) to beech data (discrete points) of Weichert [57] (left column) and Engelhardt [52] (right column)

on heat of wetting of wood, and the spruce sorption isotherm data of Weichert [57], which was recently identified as one of a select few publications giving reliable sorption data for wood at multiple temperatures [61].

Curve fits for the CAST model, GAB6 model, and NA6 model to sorption data for beech are plotted in Fig. 7, with residuals in modeled water activity plotted in Fig. 8. Curve fits for spruce sorption data are shown in SI Part VIII. The exceptional goodness of fit of the CAST model to sorption data across the wide range of temperatures is evident. Although nonrandom patterns in the residuals are evident in Fig. 8, they are less pronounced for the CAST model than the GAB6 and NA6 models. The GAB6 and NA6 models give lower R^2 values than the CAST model for both beech and spruce across all quantities, with one exception in each case. The primary disadvantage of the GAB6 model is that it does not allow analytical integration for calculating the heat of wetting. Thus, while the GAB6 model is useful for interpolation of sorption data over much of the RH range, it is not as versatile for thermodynamic modeling as the CAST model. The NA6 model statistics for spruce are consistently good and overall better than for beech, though this model does not fit the low a_w region well, particularly with increasing temperature. This may imply that the NA6 model is better suited to a limited temperature range.

The fitting statistics for the OC3 and ODE4 models are clearly inferior to those for the CAST model, although this would be expected given that they have only three or four parameters, respectively. A drawback of the linear temperature dependence in the OC3 model is that extrapolation to higher temperatures may yield nonphysical negative values of u. The ODE4 model also gives negative u values at low a_w, particularly with increasing temperature. The ODE4 model captures the general shape of the heat of wetting and the differential enthalpy of sorption (SI Part VI) but does not reproduce the effect of temperature nearly as well as the CAST model.

Although the ODP6 model generally fits the data more accurately than the ODE4 model (with two exceptions), it does not fit sorption data well at the low and high regions

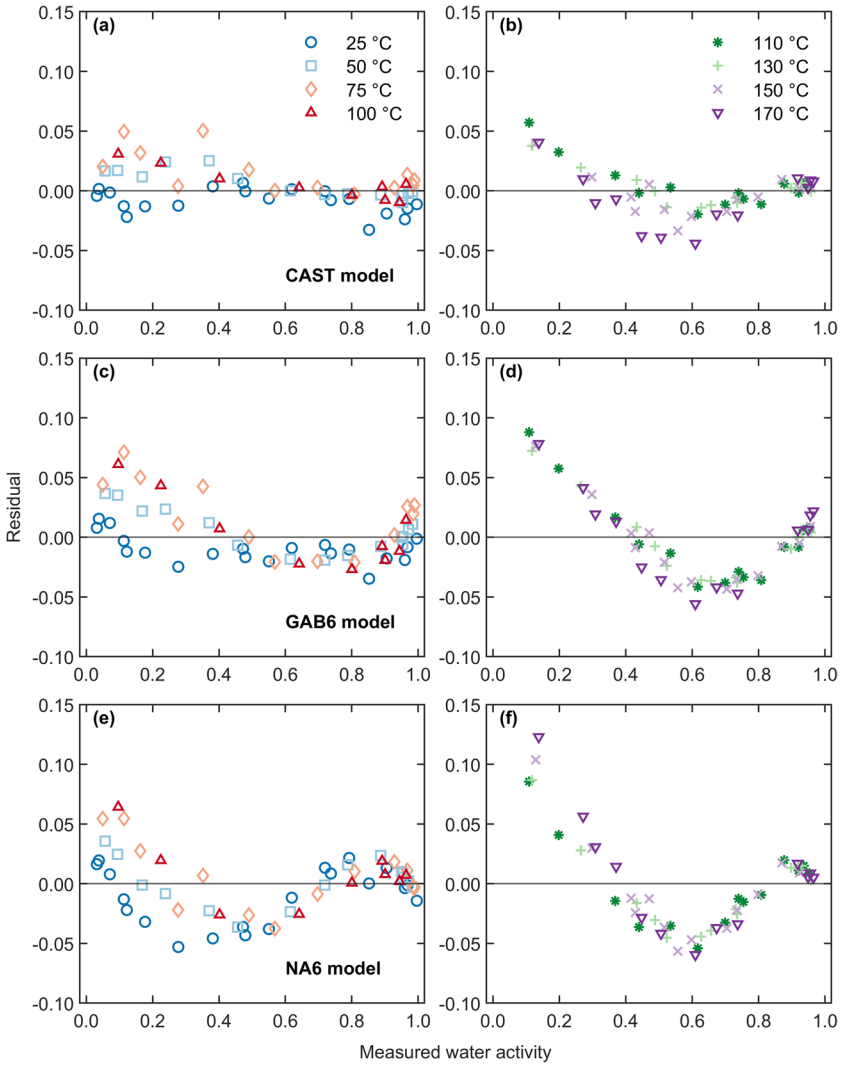

Fig. 8 Residuals in modeled water activity based on fits from Fig. 7

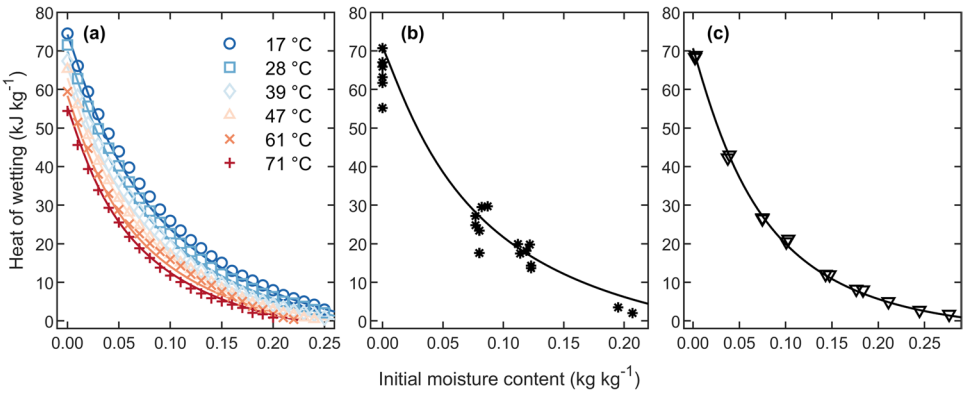

Fig. 9 Heat of wetting vs. initial moisture content from the CAST model (solid curves) fit to data (discrete points) of **a** Hearmon and Burcham [64] for beech at a series of temperatures, **b** Nopens et al. [35] for beech at 25 °C, and **c** Volbehr [63] for spruce at 0 °C

(SI Part VI). In all cases but one, the statistics for the CAST model are superior to those for the ODP6 model.

5.2 Heat of wetting

The heat of wetting given by the CAST model is plotted in Fig. 9a with experimental data for beech [64] for a series of temperatures as a function of initial moisture content. The ability of the model to replicate the shape of the data across a wide range of moisture contents and temperatures is noteworthy. The data of Nopens et al. [35] for beech at 25 °C is plotted in Fig. 9b. Although the calorimetric data exhibit considerable scatter, the CAST model represents the shape correctly. The heat of wetting of spruce at

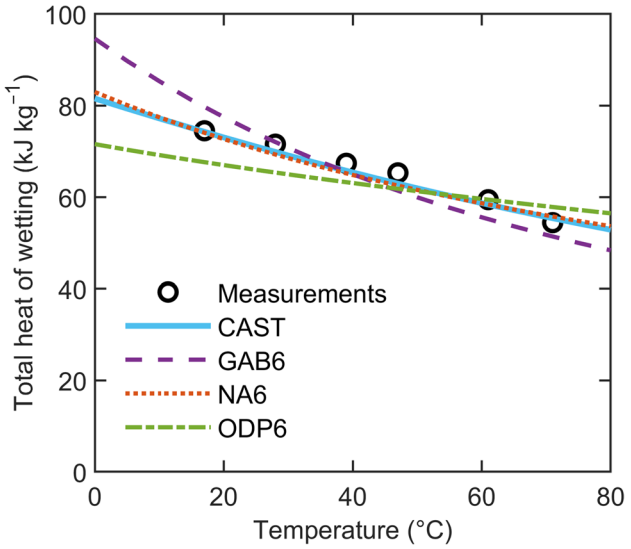

Fig. 10 Variation of the total heat of wetting of beech with temperature given by various models compared with measurements of Hearmon and Burcham [64]

0 °C [63] is plotted in Fig. 9c, with negligible deviation between model and experimental data. The CAST model thus provides exceptional agreement with both calorimetric data and sorption isotherm data across a broad range of temperatures.

The influence of temperature on the total heat of wetting for select models for beech is shown in Fig. 10. The CAST and NA6 model curves are clearly consistent with the data of Hearmon and Burcham [64]. The slopes of these curves are also consistent with calorimetric measurements for Klinki pine [66] and Hinoki [67], which found that the total heat of wetting decreases with increasing temperature at a rate of approximately −0.4 to −0.3 kJ kg_{ds}^{-1} K^{-1}. On the other hand, the GAB6 and ODP6 models do not fit the data as well. Given the lack of data for the influence of temperature on the heat of wetting of spruce (only 0 °C data), the model fitting of spruce data was not constrained to reproduce the slope observed for the other wood species. The total heat of wetting of spruce measured by Volbehr [63] at 0 °C is lower than would be expected based on the temperature dependence of the other woods. This may be a result of different sample preparation methods. For spruce, the CAST model fitting yielded a temperature dependence of the total heat of wetting of +0.10 kJ kg_{ds}^{-1} K^{-1} at 30 °C.

5.3 Differential enthalpy and entropy of sorption

The differential enthalpy of sorption given by the CAST model is compared in Fig. 11a with values reported by Weichert [65] for spruce and beech at 62.5 °C from analysis using the Clausius-Clapeyron equation and in Fig. 11b with sorption calorimetry data from Nopens et al. [35] for beech at 25 °C. The model correctly represents the shape of the data, and discrepancies are mostly within experimental uncertainty.

The differential enthalpy of sorption predicted by the CAST model at 25 °C is plotted vs. the differential entropy in Fig. 12, for the range of u values of beech and spruce corresponding to those measured by Weichert [57]. The linearity over most of the range indicates that the model is nearly in agreement with literature describing enthalpy-entropy compensation for water vapor sorption in various cellulosic materials [20, 85–90]. Departures from linearity in Fig. 12 are evident for larger values of $\Delta\bar{h}$ and $\Delta\bar{s}$, which correspond with $u < 0.04$ kg kg^{-1}. A linear relationship between $\Delta\bar{h}$ and $\Delta\bar{s}$ was not imposed on the CAST model because it is not clear that a fundamental theoretical basis for this exists. In a recent review of enthalpy-entropy compensation, Khrapunov [91] argued that the linear relationship may arise from correlated errors in enthalpy and entropy and recommended that these errors be quantified.

None of the studies cited above included uncertainty analysis. However, Thybring et al. [24] used the Monte Carlo method to determine the uncertainty in the differential enthalpy of sorption calculated from the data of Weichert [57] using the Clausius-Clapeyron equation. This work

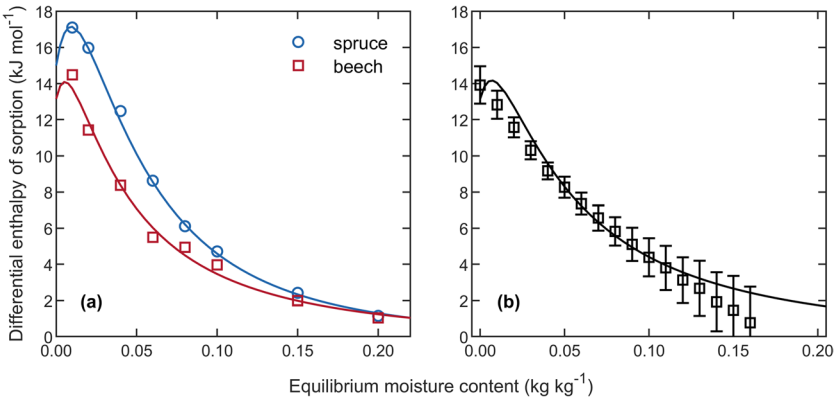

Fig. 11 Differential enthalpy of sorption vs. equilibrium moisture content from the CAST model (solid curves) compared with values (discrete points) reported by **a** Weichert [65] at 62.5 °C and **b** Nopens et al. [35] at 25 °C, where error bars indicate standard deviation of three replicates

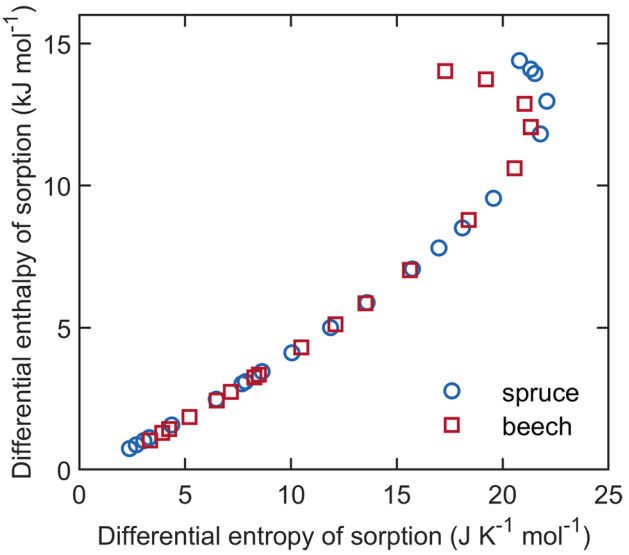

Fig. 12 Enthalpy-entropy plot for the CAST model fit to data at 25 °C [57]

showed that uncertainty in $\Delta\bar{h}$ increases appreciably with decreasing u. Although the study did not discuss enthalpy-entropy compensation, it suggests that further work is needed to assess the uncertainties in $\Delta\bar{g}$, $\Delta\bar{h}$, and $\Delta\bar{s}$ at low u and evaluate any correlation. In SI Part VI, we show that linear enthalpy-entropy compensation is a direct consequence of Othmer's postulate. But as shown previously, the models derived from Othmer's postulate do not fit the data as accurately as the CAST model.

5.4 Properties near saturation

Equilibrium moisture content curves at $a_w = 0.995$ for the various model fits to beech data are plotted as a function of temperature in Fig. 13a. The CAST model and GAB6 model show similar curves, with the NA6 model offset to slightly higher EMC. These models have the advantage of avoiding nonphysical negative u values at higher temperatures. The linear fit of Pearson et al. [62] to literature data for various wood species near 100% relative humidity is shown for comparison. This linear fit should be treated with caution given the experimental challenges with measurements at high temperature and relative humidity discussed by Pearson et al. [62], the use of extrapolation, the number of different wood species represented, and the inclusion of data that are now known to be unreliable, i.e., historic data from the Forest Products Laboratory [77].

Absorbed water in the material has thermodynamic properties very close to pure water as the water activity approaches unity. The differential enthalpy of sorption would thus be expected to approach zero. The predicted $\Delta\bar{h}$ at $a_w = 0.995$ (corresponding to high EMC) is plotted

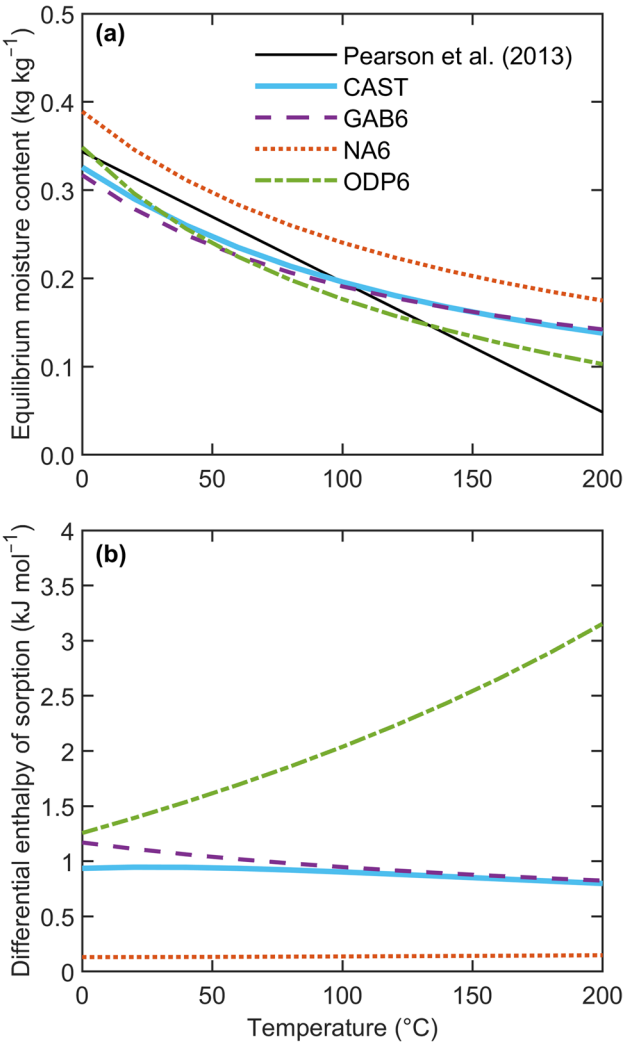

Fig. 13 **a** Equilibrium moisture content at $a_w = 0.995$ as a function of temperature from model fits to beech data, and linear fit of Pearson et al. [62] to literature data near 100% RH; **b** Differential enthalpy of sorption at $a_w = 0.995$ as a function of temperature

in Fig. 13b as a function of temperature for select models. The magnitude of $\Delta\bar{h}$ for the CAST model (< 1 kJ mol^{-1}) is small relative to the magnitude at low EMC shown in Fig. 11 (~ 14 kJ mol^{-1}) and does not vary appreciably with temperature. This may reflect a cancellation of two phenomena: EMC decreases as temperature increases (Fig. 13a) while $\Delta\bar{h}$ increases as EMC decreases (Fig. 11). For applications where sorption modeling is used in simulation of coupled heat and moisture transfer, it may be advantageous for $\Delta\bar{h}$ to be small but nonzero for computational robustness. The GAB6 model curve is similar to the CAST model, whereas the NA6 model has a lower magnitude. In contrast, the ODP6 model has a higher magnitude that increases considerably with temperature.

Although the CAST model is not intended for fitting $a_w > 0.995$, it provides a convenient way of normalizing the

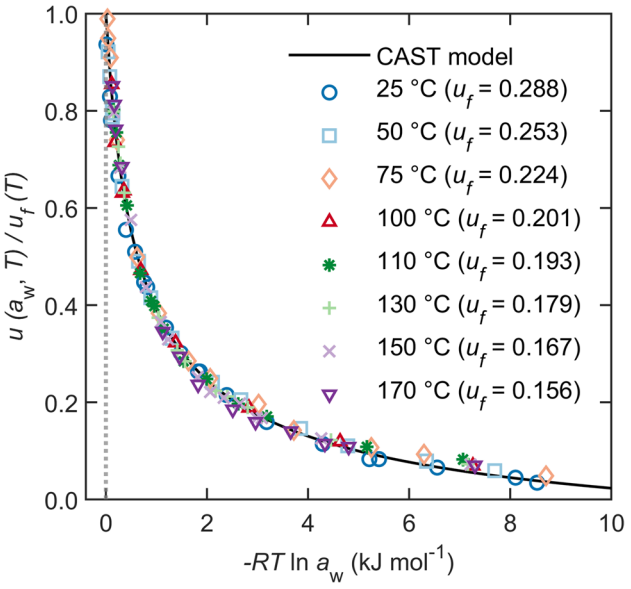

Fig. 14 Normalized equilibrium moisture content vs. differential Gibbs energy of sorption for the CAST model and beech data of Engelhardt [52] and Weichert [57]

EMC, as given by Eq. (28). The normalized EMC is plotted as a function of $\Delta\overline{g} = -RT \ln a_w$ in Fig. 14 for the CAST model and experimental beech data. Other sorption models are not included in Fig. 14 because none of them gives normalized EMC as a function of $-RT \ln a_w$ alone. The difference between $u\left(a_w = 0.995, T\right)$ shown in Fig. 13a and $u_f(T)$ is generally less than 0.008 kg kg^{-1}. This method of plotting the data yields a single curve over a range of temperatures, as shown previously by Willems [60] across several datasets for water vapor sorption in wood. However, we point out several differences. First, the experimental values in Fig. 14 are normalized by $u_f(T)$ calculated from Eq. (25) at each temperature (indicated in the legend). The constants $\beta_1 \ldots \beta_6$ used for calculating $u_f(T)$ are optimized by simultaneously fitting all the experimental quantities listed in Table 2; this includes calorimetric data in addition to sorption data. In contrast, Willems [60] used a different extrapolation method for the corresponding value, denoted $\mathrm{EMC}_{\max}$ in that work, which relied on sorption data alone; see Willems [92] for further details. Second, the universality of the relationship shown in Fig. 14 covers a wider range of temperatures; the highest temperature here is 170 °C as opposed to 100 °C in Willems [60]. Third, the thermodynamic water activity is used here instead of relative humidity.

6 Conclusions

This article clarifies the thermodynamics of water vapor sorption in cellulosic materials and formulates a new model that seamlessly links equilibrium sorption data with multiple thermodynamic quantities. We overcome two main limitations of prior work: (i) reliance on the ideal gas equation and (ii) lack of consistency between different aspects of sorption theory, often reflected in discrepancies between model predictions and independently measured thermodynamic properties.

We formulate a new model known as the Comprehensive Analytical Sorption Thermodynamic (CAST) model that is consistent with the thermodynamic framework advanced in this article. An empirical relationship between the differential Gibbs energy of sorption ($\Delta\overline{g}$), equilibrium moisture content (u), and temperature (T) serves to generate analytical equations for the differential enthalpy of sorption ($\Delta\overline{h}$), the differential entropy of sorption ($\Delta\overline{s}$), and the integral heat of wetting (q_{wet}). The fundamental relationship between $\Delta\overline{g}$ and water activity (a_w) yields a six-parameter equilibrium sorption model that can be expressed as $u(a_w, T)$ or inverted to give $a_w(u, T)$. The CAST model is evaluated using sorption data and calorimetric data from the wood science literature over a wide range of temperatures. It fits the experimental data with higher accuracy than several other models, including the six-parameter modified GAB model. Although the experimental datasets are from disparate literature sources spanning many decades, they are unified effectively by the CAST model. The relatively simple analytical equations of the CAST model provide accurate values over a wide range of temperature and moisture conditions, making it simple to implement in computer simulations of heat and moisture transfer.

Supplementary Information The online version contains supplementary material available at https://doi.org/10.1007/s10450-024-00495-2.

Acknowledgements This work was supported by the U.S. Department of Agriculture, Forest Service, Forest Products Laboratory (FPL). The authors are grateful to Martin Nopens (University of Hamburg) and coauthors for sharing calorimetric data. We thank Emil Engelund Thybring (University of Copenhagen), Joseph Jakes (FPL), Kara Yedinak (FPL), and anonymous reviewers for critical comments that improved the clarity of the article. M.D. extends appreciation to those who made prior contributions to sorption thermodynamics and offered encouragement, particularly the late Christen Skaar and former FPL colleagues William Simpson and Daniel Caulfield.

Author contributions Conceptualization: Mark A. Dietenberger; Formal analysis: Mark A. Dietenberger, Samuel V. Glass; Investigation: Mark A. Dietenberger, Samuel V. Glass, Charles R. Boardman; Methodology: Mark A. Dietenberger, Samuel V. Glass; Project administration: Mark A. Dietenberger, Samuel V. Glass; Validation: Mark A. Dietenberger, Samuel V. Glass; Visualization: Samuel V. Glass, Mark A. Dietenberger; Writing - original draft preparation: Mark A. Dietenberger, Samuel V. Glass; Writing - review and editing: Mark A. Dietenberger, Samuel V. Glass, Charles R. Boardman.

Funding This work was supported by the U.S. Department of Agriculture, Forest Service.

Data availability No datasets were generated or analysed during the current study. This study relied on literature data for model evaluation

(Table 2). Previously published data that were digitized for this study are available upon request.

Declarations

Ethics approval and consent to participate This study did not involve human or animal participants.

Consent for publication All authors agreed with the content and gave explicit consent to submit this article.

Competing interests The authors declare no competing interests.

References

1. Tiemann, H.D.: Effect of Moisture upon the Strength and Stiffness of wood. Bulletin 70. U.S. Department of Agriculture, Forest Service, Washington (1906)
2. Dunlap, F.: The specific heat of wood. U.S. Department of Agriculture, Forest Service Bulletin 110, Washington. (1912)
3. MacLean, J.D.: Thermal conductivity of wood. Heat. Pip. Air Cond. **13**(6), 380–391 (1941)
4. Glass, S.V., Zelinka, S.L.: Moisture relations and physical properties of wood (Ch. 4). In: Wood handbook—wood as an engineering material. General Technical Report FPL-GTR-282. U.S. Department of Agriculture, Forest Service, Forest Products Laboratory, Madison. (2021). https://www.fs.usda.gov/research/treesearch/62243. Accessed 30 May 2024
5. Stamm, A.J.: Wood and Cellulose Science. Ronald Press Company, New York (1964)
6. Zelinka, S.L.: Corrosion of metals in wood products (Ch. 23). In: Aliofkhazraei M (ed.), Developments in corrosion protection, InTech, ISBN 978-953-51-1223-5. (2014). https://doi.org/10.5772/57296
7. Chirife, J., del Pilar Buera, M., Labuza, T.P.: Water activity, water glass dynamics, and the control of microbiological growth in foods. Crit. Rev. Food Sci. Nutr. **36**(5), 465–513 (1996). https://doi.org/10.1080/10408399609527736
8. Gradeci, K., Labonnote, N., Time, B., Köhler, J.: Mould growth criteria and design avoidance approaches in wood-based materials – a systematic review. Constr. Build. Mater. **150**, 77–88 (2017). https://doi.org/10.1016/j.conbuildmat.2017.05.204
9. Lepage, R., Glass, S.V., Knowles, W., Mukhopadhyaya, P.: Biodeterioration models for building materials: Critical review. J. Archit. Eng. **25**(4), 04019021 (2019). https://doi.org/10.1061/(ASCE)AE.1943-5568.0000366
10. Brischke, C., Alfredsen, G.: Wood-water relationships and their role for wood susceptibility to fungal decay. Appl. Microbiol. Biotechnol. **104**, 3781–3795 (2020). https://doi.org/10.1007/s00253-020-10479-1
11. Griffin, D.M.: Water potential and wood-decay fungi. Annu. Rev. Phytopathol. **15**, 319–329 (1977). https://doi.org/10.1146/annurev.py.15.090177.001535
12. Anderson, H.E.: Predicting equilibrium moisture content of some foliar forest litter in the Northern Rocky Mountains. Research Paper INT-429, U.S. Department of Agriculture. Forest Service, Intermountain Research Station, Ogden. (1990). https://digitalcommons.usu.edu/govdocs_forest/56/. Accessed 30 May 2024
13. Nelson, R.M.: Water relations of forest fuels (Ch. 4). In: Johnson EA, Miyanishi K (eds.), Forest Fires: Behavior and Ecological Effects, Academic Press, 79–149. (2001). https://doi.org/10.1016/B978-0-123-86660-8.X5000-4
14. Viney, N.R.: A review of fine fuel moisture modelling. Int. J. Wildland Fire. **1**(4), 215–234 (1991). https://doi.org/10.1071/WF9910215
15. Dietenberger, M.A., Boardman, C.R., Weise, D.R.: Heats for combustion, capacities, and evaporation of fresh leaves, and their relationships to leaf compositions. In: Proceedings, 6th International Fire Behavior and Fuels Conference. International Association of Wildland Fire, Missoula. (2019). https://www.fs.usda.gov/treesearch/pubs/58575. Accessed 30 May 2024
16. Dietenberger, M.A., Boardman, C.R., Shotorban, B., Mell, W., Weise, D.R.: Thermal degradation modeling of live vegetation for fire dynamic simulator. In: Proceedings, 2020 Spring Technical Meeting, Central States Section of the Combustion Institute. (2020). https://www.fs.usda.gov/treesearch/pubs/60852. Accessed 30 May 2024
17. Dietenberger, M.A., Hasburgh, L.E., Yedinak, K.M.: Fire safety of wood construction (Ch. 18). In: Wood handbook—wood as an engineering material. General Technical Report FPL-GTR-282. U.S. Department of Agriculture, Forest Service, Forest Products Laboratory, Madison. (2021). https://www.fs.usda.gov/research/treesearch/62268. Accessed 30 May 2024
18. Smith, J.M., Van Ness, H.C., Abbott, M.M., Swihart, M.T.: Introduction to Chemical Engineering Thermodynamics, 9th edn. McGraw Hill, New York (2022)
19. Al-Muhtaseb, A.H., McMinn, W.A.M., Magee, T.R.A.: Moisture sorption isotherm characteristics of food products: A review. Food Bioprod. Process. **80**(2), 118–128 (2002). https://doi.org/10.1205/09603080252938753
20. Basu, S., Shivhare, U.S., Mujumdar, A.S.: Models for sorption isotherms for foods: A review. Drying Technol. **24**(8), 917–930 (2006). https://doi.org/10.1080/07373930600775979
21. Chirife, J., Iglesias, H.A.: Equations for fitting water sorption isotherms of foods: Part 1 – a review. Int. J. Food Sci. Technol. **13**(3), 159–174 (1978). https://doi.org/10.1111/j.1365-2621.1978.tb00792.x
22. Simpson, W.T.: Sorption theories applied to wood. Wood Fiber. **12**(3), 183–195 (1980)
23. Skaar, C.: Wood-water relations. Springer, New York (1988). https://doi.org/10.1007/978-3-642-73683-4
24. Thybring, E.E., Boardman, C.R., Zelinka, S.L., Glass, S.V.: Common sorption isotherm models are not physically valid for water in wood. Colloids Surf. A Physicochem. Eng. Asp. **627**(2), 127214 (2021). https://doi.org/10.1016/j.colsurfa.2021.127214
25. Thybring, E.E., Fredriksson, M., Zelinka, S.L., Glass, S.V.: Water in wood: A review of current understanding and knowledge gaps. Forests. **13**, 2051 (2022). https://doi.org/10.3390/f13122051
26. van den Berg, C., Bruin, S.: Water activity and its estimation in food systems: theoretical aspects. In: Rockland LB, Stewart GF (eds.), Water Activity: Influences on Food Quality, Academic Press, 1981, ISBN 9780125913508, 1–61. (1981). https://doi.org/10.1016/B978-0-12-591350-8.50007-3
27. Venkateswaran, A.: Sorption of aqueous and nonaqueous media by wood and cellulose. Chem. Rev. **70**(6), 619–637 (1970). https://doi.org/10.1021/cr60268a001
28. Willems, W.: A critical review of the multilayer sorption models and comparison with the sorption site occupancy (SSO) model for wood moisture sorption isotherm analysis. Holzforschung. **69**(1), 67–75 (2015). https://doi.org/10.1515/hf-2014-0069
29. Esteban, L.G., de Palacios, P., Fernández, F.G., Guindeo, A., Cano, N.N.: Sorption and thermodynamic properties of old and new *Pinus sylvestris* wood. Wood Fiber Sci. **40**(1), 111–121 (2008)
30. McMinn, W.A.M., Magee, T.R.A.: Thermodynamic properties of moisture sorption of potato. J. Food Eng. **60**(2), 157–165 (2003). https://doi.org/10.1016/S0260-8774(03)00036-0

31. Rhim, J.W., Lee, J.H.: Thermodynamic analysis of water vapor sorption isotherms and mechanical properties of selected paper-based food packaging materials. J. Food Sci. **74**(9), E502–E511 (2009). https://doi.org/10.1111/j.1750-3841.2009.01373.x
32. Simal, S., Femenia, A., Castell-Palou, A., Rosselló, C.: Water desorption thermodynamic properties of pineapple. J. Food Eng. **80**, 1293–1301 (2007). https://doi.org/10.1016/j.jfoodeng.2006.10.001
33. Chen, C.: Obtaining the isosteric sorption heat directly by sorption isotherm equations. J. Food Eng. **74**(2), 178–185 (2006). https://doi.org/10.1016/j.jfoodeng.2005.01.041
34. Leuk, P., Schneeberger, M., Hirn, U., Bauer, W.: Heat of sorption: A comparison between isotherm models and calorimeter measurements of wood pulp. Drying Technol. **34**(5), 563–573 (2016). https://doi.org/10.1080/07373937.2015.1062391
35. Nopens, M., Wadsö, L., Ortmann, C., Fröba, M., Krause, A.: Measuring the heat of interaction between lignocellulosic materials and water. Forests. **10**(8), 674 (2019). https://doi.org/10.3390/f10080674
36. Pang, S., Langrish, T.A.G., Keey, R.B.: The heat of sorption of timber. Drying Technol. **11**(5), 1071–1080 (1993). https://doi.org/10.1080/07373939308916883
37. Anderson, N.T., McCarthy, J.L.: Two-parameter isotherm equation for fiber-water systems. Industrial Eng. Chem. Process. Des. Dev. **2**(2), 103–105 (1963). https://doi.org/10.1021/i260006a003
38. Chung, D.S., Pfost, H.B.: Adsorption and desorption of water vapor by cereal grains and their products part II: Development of the general isotherm equation. Trans. ASAE. **10**(4), 552–555 (1967). https://doi.org/10.13031/2013.39727
39. Nelson, R.M.: A model for sorption of water vapor by cellulosic materials. Wood Fiber Sci. **15**(1), 8–22 (1983)
40. Hunter, A.J.: On the basic equation of sorption and the isosteric heat. Wood Sci. Technol. **25**, 99–111 (1991). https://doi.org/10.1007/BF00226810
41. Myers, A.L., Monson, P.A.: Physical adsorption of gases: The case for absolute adsorption as the basis for thermodynamic analysis. Adsorption. **20**(4), 591–622 (2014). https://doi.org/10.1007/s10450-014-9604-1
42. Adkins, C.J.: Change of phase (Ch. 10). In: Equilibrium Thermodynamics. McGraw-Hill, London (1968)
43. Ott, J.B., Boerio-Goates, J.: Chemical Thermodynamics: Principles and Applications. Elsevier Academic, San Diego (2000). https://doi.org/10.1016/B978-0-12-530990-5.X5000-7
44. Cohen, E.R., Cvitaš, T., Frey, J.G., Holmström, B., Kuchitsu, K., Marquardt, R., Mills, I., Pavese, F., Quack, M., Stohner, J., Strauss, H.L., Takami, M., Thor, A.J.: Quantities, Units and Symbols in Physical Chemistry, 3rd edn. International Union of Pure and Applied Chemistry (2007)
45. IAPWS: R6-95, Revised Release on the IAPWS Formulation 1995 for the Thermodynamic Properties of Ordinary Water Substance for General and Scientific Use. Int. Ass. Properties Water Steam (2018). http://www.iapws.org/relguide/IAPWS-95.html. Accessed 30 May 2024
46. Lemmon, E.W., Bell, I.H., Huber, M.L., McLinden, M.O.: Thermophysical properties of fluid systems. In: Linstrom, P.J., Mallard, W.G. (eds.) NIST Chemistry WebBook, NIST Standard Reference Database Number 69. National Institute of Standards and Technology, Gaithersburg (2022). https://doi.org/10.18434/T4D303
47. Wagner, W., Pruss, A.: The IAPWS Formulation 1995 for the thermodynamic properties of ordinary water substance for general and scientific use. J. Phys. Chem. Ref. Data. **31**(2), 387–535 (2002). https://doi.org/10.1063/1.1461829
48. Wagner, W., Pruss, A.: International equations for the saturation properties of ordinary water substance. Revised according to the International temperature scale of 1990. Addendum to J. Phys. Chem. Ref. Data 16, 893 (1987). J. Phys. Chem. Ref. Data. **22**(3), 783–787 (1993). https://doi.org/10.1063/1.555926
49. Othmer, D.F., Chen, H.-T.: Correlating and predicting thermodynamic data—reference substance equations and plots. Ind. Eng. Chem. **60**(4), 39–61 (1968). https://doi.org/10.1021/ie50700a007
50. Anonymous: Two simple yet accurate equations for calculating the fugacity coefficient phi and the gas compressibility factor Z. (2020). https://mychemengmusings.wordpress.com/2020/11/16/two-simple-yet-accurate-equations-for-calculating-the-fugacity-coefficient-phi-and-the-gas-compressibility-factor-z/. Accessed 30 May 2024
51. Myers, A.L.: Thermodynamics of adsorption in porous materials. AIChE J. **48**(1), 145–160 (2002). https://doi.org/10.1002/aic.690480115
52. Engelhardt, F.: Untersuchungen über die Wasserdampfsorption Durch Buchenholz Im Temperaturbereich Von 110 bis 170°C (investigations on the sorption of water vapor by beech in the temperature range 110 to 170°C). Holz als Roh- und Werkst. **37**, 99–112 (1979). https://doi.org/10.1007/BF02610854
53. Halsey, G.: Physical adsorption on non-uniform surfaces. J. Chem. Phys. **16**(10), 931–937 (1948). https://doi.org/10.1063/1.1746689
54. Weisser, H.: Influence of temperature on sorption equilibria. In: Simatos D, Multon JL (eds.), Properties of water in foods. NATO ASI Series, 90: 95–117. Springer, Dordrecht, (1985). https://doi.org/10.1007/978-94-009-5103-7_7
55. Urquhart, A.R., Williams, A.M.: The moisture relations of cotton ii.—The absorption and desorption of water by soda-boiled cotton at 25°C. J. Text. Inst. Trans. **15**(9), T433–T442 (1924). https://doi.org/10.1080/19447022408661314
56. Zeller, S.M.: Humidity in relation to moisture imbibition by wood and to spore germination on wood. Ann. Mo. Bot. Gard. **7**(1), 51–74 (1920). https://doi.org/10.2307/2990045
57. Weichert, L.: Untersuchungen über das Sorption- Und Quellungsverhalten Von Fichte, Buche Und Buchen-Preßvollholz Bei Temperaturen Zwischen 20° und 100°C (investigations on sorption and swelling of spruce, beech and compressed beech wood at temperatures between 20° and 100°C). Holz als Roh-und Werkst. **21**, 290–300 (1963a). https://doi.org/10.1007/BF02610962
58. Hedlin, C.P.: Sorption isotherms of twelve woods at subfreezing temperatures. For. Prod. J. **17**, 43–48 (1967)
59. Fredriksson, M.: On wood–water interactions in the over-hygroscopic moisture range—mechanisms, methods, and influence of wood modification. Forests. **10**(9), 779 (2019). https://doi.org/10.3390/f10090779
60. Willems, W.: Hygroscopic wood moisture: Single and dimerized water molecules at hydroxyl-pair sites? Wood Sci. Technol. **52**, 777–791 (2018). https://doi.org/10.1007/s00226-018-0998-x
61. Zelinka, S.L., Glass, S.V., Thybring, E.E.: Evaluation of previous measurements of water vapor sorption in wood at multiple temperatures. Wood Sci. Technol. **54**, 769–786 (2020). https://doi.org/10.1007/s00226-020-01195-0
62. Pearson, H., Gabbitas, B., Ormarsson, S.: Equilibrium moisture content of radiata pine at elevated temperature and pressure reveals measurement challenges. J. Mater. Sci. **48**, 332–341 (2013). https://doi.org/10.1007/s10853-012-6750-2
63. Volbehr, B.F.K.J.: Untersuchungen über die Quellung der Holzfaser (Investigations of the swelling of wood fibers). Dissertation, Kiel University, Germany. (1896)
64. Hearmon, R.F.S., Burcham, J.N.: The specific heat and heat of wetting of wood. Chem. Ind. **31**, 807–808 (1956)
65. Weichert, L.: Untersuchungen über das Sorptions- und Quellungsverhalten von Fichte, Buche und Buchen-Pressvollholz bei Temperaturen zwischen 20°C und 100°C (Investigations on sorption and swelling of spruce, beech and compressed beech wood at temperatures between 20°C and 100°C). Dissertation, Faculty of

Mechanical and Electrical Engineering, Technical University of Munich, Germany. (1963)
66. Kelsey, K.E., Clarke, L.N.: The heat of sorption of water by wood. Aust. J. Appl. Sci. **7**(2), 160–175 (1956)
67. Kajita, H.: The heat of wetting of wood in water. Bull. Kyoto Prefectural Univ. Forests. **20**, 49–61 (1976)
68. Guggenheim, E.A.: Chap. 11. Localized monolayer and multilayer adsorption of gases. In: Applications of Statistical Mechanics, pp. 186–206. Clarendon, Oxford (1966)
69. Anderson, R.B.: Modifications of the Brunauer, Emmett and Teller equation. J. Am. Chem. Soc. **68**(4), 686–691 (1946). https://doi.org/10.1021/ja01208a049
70. de Boer, J.H.: The quantity σ: Unimolecular and multimolecular adsorption (Ch. 5). In: The Dynamical Character of Adsorption, pp. 54–89. Clarendon, Oxford (1953)
71. Ramarao, B.V.: Moisture sorption and transport processes in paper materials. In: Dąbrowski A (ed.), Studies in Surface Science and Catalysis, Volume 120, Part A (Adsorption and its Applications in Industry and Environmental Protection), 531–560. (1999). https://doi.org/10.1016/S0167-2991(99)80564-3
72. Singh, P.C., Singh, R.K.: Application of GAB model for water sorption isotherms of food products. J. Food Process. Preserv. **20**(3), 203–220 (1996). https://doi.org/10.1111/j.1745-4549.1996.tb00743.x
73. Oswin, C.R.: The kinetics of package life. III. The isotherm. J. Soc. Chem. Ind. **65**(12), 419–421 (1946). https://doi.org/10.1002/jctb.5000651216
74. Chen, C.: A study of equilibrium relative humidity for yellow-dent corn kernels. Dissertation, University of Minnesota, USA. (1988)
75. Chen, C., Morey, R.V.: Comparison of four EMC/ERH equations. Trans. ASAE. **32**(3), 983–990 (1989). https://doi.org/10.13031/2013.31103
76. Kaleemullah, S., Kailappan, R.: Moisture sorption isotherms of red chillies. Biosyst. Eng. **88**(1), 95–104 (2004). https://doi.org/10.1016/j.biosystemseng.2004.01.003
77. Glass, S.V., Zelinka, S.L., Johnson, J.A.: Investigation of historic equilibrium moisture content data from the Forest Products Laboratory. General Technical Report FPL-GTR-229. Department of Agriculture, Forest Service, Forest Products Laboratory, Madison. (2014). https://doi.org/10.2737/FPL-GTR-229
78. Boardman, C.R., Glass, S.V.: Moisture transfer through the membrane of a cross-flow energy recovery ventilator: Measurement and simple data-driven modeling. J. Building Phys. **38**(5), 389–418 (2015). https://doi.org/10.1177/1744259113506072
79. Othmer, D.F.: Correlating vapor pressure and latent heat data. Ind. Eng. Chem. **32**(6), 841–856 (1940). https://doi.org/10.1021/ie50366a022
80. Othmer, D.F., Sawyer, F.G.: Correlating adsorption data. Ind. Eng. Chem. **35**(12), 1269–1276 (1943). https://doi.org/10.1021/ie50408a012
81. Aguerre, R.J., Suárez, C., Viollaz, P.E.: The temperature dependence of isosteric heat of sorption of some cereal grains. Int. J. Food Sci. Technol. **23**(2), 141–145 (1988). https://doi.org/10.1111/j.1365-2621.1988.tb00560.x
82. Falabella, M.C., Aguerre, R.J., Suárez, C.: Determination of the heat of water vapor sorption by means of electronic hygrometers. Lebensm.-Wiss. Technol. **22**, 11–14 (1989)
83. Gallaher, G.L.: A method of determining the latent heat of agricultural crops. Agricultural Eng. **32**(1), 34–38 (1951)
84. Hunter, A.J.: An isostere equation for some common seeds. J. Agric. Eng. Res. **37**(3–4), 93–105 (1987). https://doi.org/10.1016/S0021-8634(87)80008-2
85. Aguerre, R.J., Suárez, C., Viollaz, P.E.: Enthalpy-Entropy compensation in sorption phenomena: Application to the prediction of the effect of temperature on food isotherms. J. Food Sci. **51**(6), 1547–1549 (1986). https://doi.org/10.1111/j.1365-2621.1986.tb13856.x
86. Avramidis, S.: Enthalpy-Entropy compensation and thermodynamic considerations in sorption phenomena. Wood Sci. Technol. **29**, 329–333 (1992). https://doi.org/10.1007/BF00226074
87. Beristain, C.I., Garcia, H.S., Azuara, E.: Enthalpy-Entropy compensation in food vapor adsorption. J. Food Eng. **30**(3–4), 405–415 (1996). https://doi.org/10.1016/S0260-8774(96)00011-8
88. Ferro Fontan, C., Chirife, J., Sancho, E., Iglesias, H.A.: Analysis of a model for water sorption phenomena in foods. J. Food Sci. **47**(5), 1590–1594 (1982). https://doi.org/10.1111/j.1365-2621.1982.tb04989.x
89. Peralta, P.N., Bangi, A.P., Lee, A.W.C.: Thermodynamics of moisture sorption by the giant-timber bamboo. Holzforschung. **51**(2), 177–182 (1997). https://doi.org/10.1515/hfsg.1997.51.2.177
90. Rawat, S.P., Khali, D.P.: Enthalpy-Entropy compensation during sorption of water in wood. J. Appl. Polym. Sci. **60**(5), 787–790 (1996). https://doi.org/10.1002/(SICI)1097-4628(19960502)60:5%3C787::AID-APP18%3E3.0.CO;2-W
91. Khrapunov, S.: The enthalpy-entropy compensation phenomenon. Limitations for the use of some basic thermodynamic equations. Curr. Protein Pept. Sci. **19**(11), 1088–1091 (2018). https://doi.org/10.2174/1389203719666180521092615
92. Willems, W.: Hydrostatic pressure and temperature dependence of wood moisture sorption isotherms. Wood Sci. Technol. **48**, 483–498 (2014). https://doi.org/10.1007/s00226-014-0616-5